Unravelling druggable signalling networks that control F508del-CFTR proteostasis

Ramanath Narayana Hegde[a,1,2], Seetharaman Parashuraman[a,*,1,2], Francesco Iorio[2,°,b], Fabiana Ciciriello[3,4,2,b], Fabrizio Capuani[2,#], Annamaria Carissimo[2], Diego Carrella[2], Vincenzo Belcastro[2], Advait Subramanian[1], Laura Bounti[1,□], Maria Persico[2], Graeme Carlile[4], Luis Galietta[5], David.Y.Thomas[4], Diego Di Bernardo[2,6], and Alberto Luini*[1,2,7].

[1]Institute of Protein Biochemistry, National Research Council, Via P. Castellino 111, 80131, Naples, Italy.

[2]Telethon Institute of Genetics and Medicine, Via Campi Flegrei 34, 80078 Pozzuoli, Italy.

[3]Biology and Biotechnology Department "Charles Darwin", Sapienza University, Rome, Italy.

[4]Biochemistry Department, McIntyre Medical Sciences Building, McGill University, 3655 Promenade Sir William Osler, Montréal, Québec H3G 1Y6, Canada.

[5]U.O.C. Genetica Medica, Institute of Giannina Gaslini, Via Gerolamo Gaslini 5, 16147 Genova, Italy.

[6]Dept. of Electrical Engineering and Information Technology, University of Naples "Federico II", Via Claudio 21, 80125, Napoli, Italy.

[7]Istituto di Ricovero e Cura a Carattere Scientifico SDN, Via Emanuele Gianturco, 113, 80143 Naples, Italy.

[°]Current address: European Molecular Biology Laboratory – European Bioinformatics Institute, Wellcome Trust Genome Campus, Cambridge CB10 1SD, UK.

[#]Current address: Physics Department, University of Rome "La Sapienza", Piazzale Aldo Moro 3, 00185 Rome, Italy.

[□]Current address: KU Leuven University, 3000 Leuven, Belgium.

[a] Co-first authors

[b] Contributed equally among them

* Corresponding authors

Running title: Signalling networks controlling proteostasis

Address correspondence to:

AL: Email: a.luini@ibp.cnr.it; Tel: +39-081-6132535; Fax: +39-081-6132277

SP: Email: r.parashuraman@ibp.cnr.it; Tel: +39-081-6132631; Fax: +39-081-6132277

Key words: Cystic fibrosis, proteostasis regulators, signalling networks, mechanism of action of drugs, CFTR

SUMMARY

Cystic fibrosis (CF) is caused by mutations in CF transmembrane conductance regulator (CFTR). The most frequent mutation (F508del-CFTR) results in altered proteostasis, i.e., in the misfolding and intracellular degradation of the protein. The F508del-CFTR proteostasis machinery and its homeostatic regulation are well studied, while the question whether 'classical' signalling pathways and phosphorylation cascades might control proteostasis remains barely explored. Here, we have unravelled signalling cascades acting selectively on the F508del-CFTR folding-trafficking defects by analysing the mechanisms of action of F508del-CFTR proteostasis regulator drugs through an approach based on transcriptional profiling followed by deconvolution of their gene signatures. Targeting multiple components of these signalling pathways resulted in potent and specific correction of F508del-CFTR proteostasis and in synergy with pharmacochaperones. These results provide new insights into the physiology of cellular proteostasis and a rational basis for developing effective pharmacological correctors of the F508del-CFTR defect.

INTRODUCTION

Cystic fibrosis (CF) is the most common lethal genetic disease in Caucasians. It is caused by mutations in the *CF transmembrane conductance regulator* (*CFTR*) gene that encodes a chloride channel localised to the apical membrane of several epithelial cells. Mutations that cause CFTR loss of function impair the transepithelial movement of salts at the cell surface, resulting in pleiotropic organ pathology and, in the lungs, in chronic bacterial infections that eventually lead to organ fibrosis and failure (Riordan, 2008).

The CFTR protein comprises two membrane-spanning domains, two cytosolic nucleotide-binding domains, and a regulatory domain, folded together into a channel (Riordan, 2008). Folding occurs in the endoplasmic reticulum (ER) through the sequential action of multiple chaperone complexes (Loo et al., 1998; Meacham et al., 1999; Rosser et al., 2008) and is followed by export out of the ER and glycosylation in the Golgi before arrival at the plasma membrane (PM), where CFTR undergoes several cycles of endocytosis before degradation in the lysosomes (Gentzsch et al., 2004). The most frequent mutant, which is present in ~90% of the CF patients, misses a phenylalanine at position 508 (F508del-CFTR) and folds in a kinetically and thermodynamically impaired fashion into a conformation that is recognized as defective by the ER quality control (ERQC) system. It is thus retained in the ER and targeted for ER-associated degradation (ERAD) by the ubiquitin–proteasome machinery (Jensen et al., 1995; Ward et al., 1995). A small fraction of F508del-CFTR may escape degradation in the ER and reach the PM, where it can function as a channel. This might have therapeutic relevance because patients that express even low levels of functional channel have milder symptoms (Amaral, 2005). However, at the PM, F508del-CFTR is recognized by the peripheral (or PM-associated) quality control (PQC) system and is rapidly degraded in the lysosomes (Okiyoneda et al., 2010).

In contrast to the fairly extensive knowledge about the machinery involved in the

proteostasis (or protein homeostasis) of F508del-CFTR, the regulatory mechanisms that operate on the F508del-CFTR proteostasis machinery remain relatively less explored. Notable exceptions are the recent studies on the effects of the unfolded protein response and heat shock response (UPR and HSR, respectively) on the proteostasis of F508del-CFTR. The UPR and HSR operate as *homeostatic* reactions that tend to redress the imbalances between the load of unfolded proteins and the folding capacity of a cell essentially by enhancing the transcription of the cellular folding machinery. Investigators have therefore sought to induce these reactions by pharmacological means with the aim to rescue the F508del-CFTR folding/transport defect, with partial success (Roth et al., 2014; Ryno et al., 2013).

Very little is known instead about the regulation of proteostasis by the 'classical' signalling networks composed of GTPases, second messengers, kinases *etc*. that are usually activated by PM receptors and control most, if not all, of the cellular functions. We and others have previously shown that constitutive trafficking along the secretory pathway is potently controlled by such signalling networks triggered by both extra- and intracellular stimuli (Cancino et al., 2014; Chia et al., 2012; De Matteis et al., 1993; Farhan et al., 2010; Giannotta et al., 2012; Pulvirenti et al., 2008; Simpson et al., 2012). This suggests that the machinery of proteostasis *viz*. protein synthesis, folding, and degradation, is also likely to be controlled by similar signalling systems. Identifying the relevant regulatory components of these systems would not only enhance our understanding of the physiology of proteostasis, but also have significant impact on future therapeutic developments, because components of the signalling cascades, such as membrane receptors and kinases, are generally druggable, and are, in fact, the main targets of most known drugs.

Thus, this study aims to uncover signalling pathways that control proteostasis of F508del-CFTR. To this end, we have developed a strategy based on the analysis of the

mechanisms of action (MOAs) of drugs that regulate the proteostasis of F508del-CFTR. The choice of this strategy over more traditional approaches such as kinome-wide screenings was based on the rationale that since many of the successful drugs target multiple molecular pathways simultaneously (Lu et al., 2012) and with limited toxicity, elucidating the MOAs of these drugs might lead to uncovering molecular networks that regulate proteostasis in a synergistic and relatively 'safe' manner.

Several drugs that regulate the proteostasis of F508del-CFTR (hereinafter referred to as proteostasis regulators) and enhance its ability to reach the PM have been identified over the years, largely through screening campaigns (Calamini et al., 2012; Carlile et al., 2012; Hutt et al., 2010). In addition, molecules that bind directly to F508del-CFTR and facilitate its folding have also been characterized (pharmacochaperones) (Calamini et al., 2012; Kalid et al., 2010; Odolczyk et al., 2013; Pedemonte et al., 2005; Sampson et al., 2011; Van Goor et al., 2006; Wang et al., 2007). Both these groups of drugs that enhance the ability of F508del-CFTR to reach the PM are referred to as correctors. The MOA of the pharmacochaperones has been partially understood (Farinha et al., 2013a; Okiyoneda et al., 2013), and they are approaching the level of effectiveness required for clinical use [(Wainwright et al., 2015) and see also http://www.fda.gov/NewsEvents/Newsroom/PressAnnouncements/ucm453565.htm], while the proteostasis regulators are presently too ineffective to be of clinical interest.

Here, we have analysed the MOAs corrector drugs that are proteostasis regulators by deconvolving their transcriptional effects. Changes in gene expression are significant components of the MOAs of many drugs (Popescu, 2003; Santagata et al., 2013), and the analysis of transcriptional MOAs is a growing research area (Iorio et al., 2010; Iskar et al., 2013). However, a major difficulty here is that the available proteostasis regulator drugs include representatives of diverse pharmacological classes such as histone deacetylase inhibitors (Hutt et al., 2010), poly(ADP-ribose) polymerase

inhibitors (Anjos et al., 2012; Carlile et al., 2012), hormone receptor activators (Caohuy et al., 2009), cardiac glycosides (Zhang et al., 2012), and others. Thus, the effects of the available F508del-CFTR correctors are most probably not mediated by their heterogeneous principal MOA, but by some unknown weak secondary MOAs ('side effects') that these drugs share. In order to extract the transcriptional changes that are correction-related from those that are due to the (correction-irrelevant) principal MOAs of the corrector drugs we have developed a new approach based on the 'fuzzy' intersection of gene expression profiles. This method, applied to a set of proteostatic correctors will identify genes that are commonly modified by these drugs and should therefore correspond to the correction-related pathways and not to their heterogeneous primary effects. Using this strategy, we harvested a group of few hundred genes that are regulated by most of the proteostatic correctors, and then derived a series of molecular networks from this gene pool through bioinformatic and experimental approaches. Several of these networks are signalling pathways made up of druggable receptors and kinases. Silencing or targeting these pathways with chemical blockers inhibit the degradation in the ER and enhance the transport of F508del-CFTR to the PM. Moreover, the large pool of ER-localised foldable F508del-CFTR that results from the inhibition of ER degradation can be acted upon by pharmacochaperones, to further enhance correction. These findings build on previous screening studies and on the accumulated knowledge of F508del-CFTR proteostasis to start to define the network of signalling pathways that control F508del-CFTR proteostasis, and thereby provide a rational basis for the development of novel, potent and specific proteostasis corrector treatments for CF.

RESULTS

Proteostasis correctors have a shared transcriptional signature

Proteostasis regulators share the ability to correct (albeit weakly) the F508del-CFTR folding-trafficking defect but have principal pharmacological effects not related to F508del-CFTR correction. If the correction-related MOAs of these drugs are transcription-dependent (see materials and methods for evidence that they are), then the gene signatures of these drugs should comprise both genes related to F508del-CFTR correction and genes related to their heterogeneous primary effects.

So we sought to analyse the transcriptional MOAs of correctors (24 drugs/conditions altogether) with different chemical structures and pharmacological activities (Table 1), excluding known pharmacochaperones. The gene signatures of 13 correctors were obtained in our laboratories using immortalised CF bronchial epithelial (CFBE41o-) cells (Kunzelmann et al., 1993) on an Agilent microarray platform (CFBE dataset; see Supplementary File 1 and GEO accession number GSE67698 for the expression profiles). Another 11 signatures were extracted from the MANTRA (Mode of action by network analysis, (Iorio et al., 2010); MANTRA dataset) that were based on the Affymetrix platform. Two drugs, glafenine and ouabain were present in both datasets. Even though the signatures of each drug in the two platforms were obtained from different cell lines, they were similar enough (not shown) to suggest that two datasets can be treated together.

To extract the correction-related transcriptional effects from those due to primary effects of the correctors, we first attempted to cluster the drugs based on commonalities in their transcriptional profiles. These attempts using classical and alternate clustering methods did not yield meaningful results (see Figure 1-figure supplement 1 and Supplementary File 2) possibly because the strong transcriptional effects of the

heterogeneous principal MOAs of these drugs obscures the potential clustering of drug signatures based on their secondary correction-relevant MOAs.

In order to detect these weak but common transcriptional signatures we developed a method based on the fuzzy intersection of transcriptional profiles (FIT) (Figure 1A). Here, the corrector gene signatures are 'intersected' to identify their commonalities and this returned a pool of genes that are potentially correction-related (CORE) and are modulated by most of the correctors. The intersections among the majority of the signatures should include the correction-related (CORE) genes but exclude genes related to the heterogeneous principal effects of the drugs. The method thus captures common MOAs but not MOAs specific for individual drugs or small groups of drugs.

The main parameters of the FIT analysis (number of correctors; number of genes to be analysed in each signature, and cut-off threshold for inclusion in the correction-relevant gene pool; see materials and methods and Figure 1B-C) were selected to identify a sufficiently large CORE gene pool for pathway analysis, and also to minimise the number of 'false' CORE genes. The FIT analysis of the gene signatures resulted in 219 downregulated and 402 upregulated CORE genes (Supplementary File 3; Figure 1D; see also materials and methods). Each of these CORE genes were shared by 70% of the corrector signatures. The number of CORE genes were 3-fold higher than that expected on a random basis (see materials and methods).

This indicates that common transcriptional programmes that might be correction-relevant are indeed embedded in the signatures of proteostasis correctors.

Identification of CORE genes/ pathways involved in F508del-CFTR correction

To understand the relation of CORE genes to CFTR proteostasis, we built a dataset of known F508del-CFTR proteostasis-relevant genes by assembling literature data

208 (Supplementary File 4) and mapped their interactions with the CORE pool using
209 STRING (Franceschini et al., 2013). We found extensive and statistically significant (see
210 materials and methods) protein-protein interactions among the nodes of the union of
211 these two datasets (Figure 1F), indicating that (at least a fraction of) the CORE genes
212 are related to CFTR proteostasis. Significant interactions were also found between the
213 CORE genes from CFBE and the MANTRA datasets (not shown) confirming they are
214 related and thus can be analysed together.

215 We next applied standard bioinformatic tools to the CORE gene pool to identify
216 functionally coherent pathways/ networks/ groups. A search proteostasis components
217 among CORE genes retrieved 48 folding/ degradation and 24 transport-machinery
218 components (Supplementary File 5), some of which are known to be involved in
219 F508del-CFTR proteostasis. However, perhaps surprisingly, they were not significantly
220 enriched, indicating that changes in the expression levels of *significant numbers* of the
221 proteostasis machinery genes is not part of the MOA of the proteostasis regulator drugs.
222 Potential explanations for this could be that some proteostasis genes that are crucial
223 enough to have a strong effect on F508del-CFTR proteostasis are indeed regulated by
224 the correctors, but are not numerous enough to result in a statistical enrichment of this
225 gene group; or that the corrector drugs act by modulating the expression of regulatory
226 genes/pathways that act post-translationally on the proteostasis machinery (see results
227 from the screening below).

228 Since our interest was in the identification of signaling networks that regulate
229 proteostasis we also searched for the presence of signalling molecules among CORE
230 genes and found 24 kinases and 6 phosphatases (Supplementary File 5). Further,
231 Ingenuity pathway analysis (IPA) tool identified several statistically significant signalling
232 networks. The IPA networks comprised also (predicted) interactors of CORE genes,
233 some of which were network hubs (Figure 1- figure supplement 2). Such hubs were

often constituents of signalling pathways such as growth-factor-mediated pathways (e.g., receptors for vascular endothelial growth factor [VEGF] and platelet-derived growth factor [PDGF], phosphatidylinositol 3-kinase [PI3K], and mitogen-activated protein kinases [MAPKs]), inflammation-associated pathways (NF-κB subunits, Toll-like receptor 4 [TLR4]), stress-activated protein kinase (SAPK) pathways [MAP2K3/6 (MKK3/6), MAP2K4/7 (MKK4/7)], and casein-kinase pathway (CSNK2A1/ CKII). These hubs might control the CORE genes. Of note, many of the hubs were frequently present in the gene signatures of the individual correctors, although below the fuzzy cut-off threshold of 0.7 required for inclusion in the CORE gene pool itself (not shown).

Analysis of the promoters of CORE genes aimed at the identification of upstream transcription factors did not generate interpretable results.

We then turned to experimental validation of the role of CORE genes in the regulation of F508del-CFTR proteostasis. Experiments were carried out using a characterised biochemical assay (See materials and methods and Figure 2- figure supplement 1 for details) that detects both the amount of core-glycosylated CFTR trapped in the ER (band B with Western blotting) and the amount of CFTR fully glycosylated in the Golgi (most of which presumably resides at the PM; band C with Western blotting). As a model system, we used non-polarised CFBE41o- cells stably expressing F508del-CFTR (Bebok et al., 2005) (hereafter referred to as CFBE); but many experiments were carried out also in HeLa, BHK and polarized CFBE cells, with results that were in good qualitative agreement with the CFBE data. While this assay is not suitable for large-scale screening, it provides quantitative information on the main proteostasis parameters including CFTR accumulation in the ER, ER-associated CFTR degradation, and transport and processing in the Golgi complex. Moreover, this assay is specific for proteostasis as it separates the effects on the F508del-CFTR protein from the effects on conductance as revealed by faster chloride-permeability assays

(Pedemonte et al., 2005). Experimental validation was restricted to a limited set of genes: downregulated CORE genes (to exploit the availability of siRNA-based downregulation and of small-molecule inhibitors) that showed functional coherence, i.e., were found in protein-protein interaction networks or in enriched GO groups; or were network hubs from Ingenuity analysis, or ubiquitin ligases and signalling molecules. In total, this resulted in a group of 108 genes (Supplementary File 3). Notably, these genes had no previously reported role in the regulation of F508del-CFTR proteostasis.

CFBE cells were treated with siRNAs against these genes and the effects on both bands B and C were monitored. As a reference for correction, we used the investigational drug VX-809 (Van Goor et al., 2006), a robust corrector that acts as a pharmacochaperone. VX-809 treatment increased band C levels by 4–5-fold over control in most experiments. In all, 47 out of the 108 genes tested were found to be active in regulating F508del-CFTR proteostasis (Figure 2A-D). Of these, 32 genes (when depleted) enhanced the levels of bands B and C by 1.5-fold to more than 10-fold over controls, while 15 genes decreased bands B and C by 20 to 80% of the control levels. We refer to these as anti-correction and pro-correction genes, respectively. Among these active genes, 30 were CORE genes and 17 were hubs in IPA networks. Notably, the correction that was induced by depletion of many anti-correction genes was greater than that achieved by VX-809 (Figure 2A), or by the corrector drugs originally included in the study (see Figure 2- figure supplement 2A). This was in particular the case for a group of four poorly characterised ubiquitin ligases (RNF215, UBXO5, ASB8, FBXO7) that were not known to regulate F508del-CFTR proteostasis. RNF215 depletion increased the levels of bands C to over 10-fold the control levels (Figure 2A). Given these strong effects, RNF215 is a worthy candidate for further studies as a potential ERAD machinery component. Also notably, the depletion of many anti-correction genes not only enhanced the bands B and C but also markedly increased (to different extents) the band C/band B ratio (Figure 2C),

suggesting that these genes affect the efficiency of export of F508del-CFTR protein from the ER and/or the stability of this protein after export. Given that siRNA treatments often have off-target effects, several controls were performed to ensure the specificity of the observed effects on proteostasis (see Methods section for details). It is also to be noted that the downregulation of anti-correction genes did not change the levels of F508del-CFTR mRNA (Figure 2- figure supplement 2B) suggesting that the observed effect is not due to increased F508del-CFTR synthesis, although these data cannot by themselves exclude an effect on translation. Further experiments confirm that the effect of the downregulation of these genes is mostly (if not completely) on F508del-CFTR degradation and folding/export (see below).

It might appear surprising to find both pro-correction and anti-correction genes within the downregulated CORE gene pool. However, these genes are, presumably, components of complex transcriptional modules whose role is to control cellular functions in a balanced manner. To this end, the concomitant operation of regulatory systems of opposite signs is probably necessary (Hart and Alon, 2013). These observations are therefore likely to be a reflection of the organization of the transcriptional programs that regulate proteostasis.

Based on the above results, we sought to identify putative pathways/ networks/ groups (collectively networks) within the 47 *active* CORE gene pool, using literature data and pathway building tools (see Figure 2E for details). This resulted in several small potential networks (each comprising 2 to 6 connected elements), 4 of which were composed of signalling molecules and will be referred to by the name of their 'central' components: MLK3 (MAP3K11), PI3K, and CKII (with predominantly anti-correction activity) and ERBB4 (with pro-correction activity). A recent kinome-wide screening (published while this manuscript was being submitted) identified several kinases that regulate the rescue of F508del-CFTR (Trzcinska-Daneluti et al., 2015), with no overlap

with the hits identified here (possibly due to the different functional assays and cell types used in that study versus ours). Other 3 of the networks shown in Figure 2 comprised spliceosome, centromere and mediator complex components; and 2 were groups of ubiquitin-ligases and kinases.

Proteostasis corrector drugs act in part by modulating the expression of CORE genes

We next sought to verify whether the effects of correctors on the CORE genes might explain the action of these drugs. We first analysed the frequency of the active CORE genes among the genes downregulated by the corrector drugs. The CORE genes were about ~3-fold enriched in the signatures of correctors compared to those of other ~200 drugs taken at random from the MANTRA database (not shown). We next searched for MANTRA drugs that significantly downregulate the CORE genes (anti-correctors) using GSEA (specifically two-tailed symmetric GSEA as implemented in MANTRA; http://mantra.tigem.it/). The top 25 hits included 3 of the correctors that we had used for the FIT analysis. From the remaining 22 we selected 8 drugs (based on availability) for testing in the correction assay. Among these, mitoxantrone was found to potently increase both band C and band B. (Figure 2F); in addition, among the top 5 hits was Vorinostat, an HDAC inhibitor that was shown to act as a corrector (Hutt et al., 2010). Thus, at least 20% (5 out of 22) of the short-listed drugs were correctors, while among a large number (>20) of randomly selected drugs none showed correction activity (not shown). These data suggest that the downregulation of CORE genes is a useful criterion to identify correctors. We then extended our analysis of the top hits by comparing the 5 active drugs with those that failed to correct and also by examining upregulated genes in their gene expression profiles. The correctors showed a high frequency (2 to 3 fold more than non-corrector drugs) of up-regulation of the potent pro-corrector genes MKK1,

MKK3 and FGFBP1 while the non-corrector drugs up-regulated more frequently (2 to 3 fold more than corrector drugs) the anti-corrector genes NF-κB2 and MKK7. These results thus suggest that considering also the upregulation of CORE genes will help in further defining the search space for new correctors.

Altogether, the above data indicate that the drug-induced modulation of CORE genes is a significant component of the MOAs of corrector drugs. Thousands of gene signatures of drugs and perturbagens are being deposited in specialized databases (http://www.lincscloud.org/). These and a more extensive search for CORE genes will provide useful tools for a more refined bioinformatic identification of new correctors.

Epistatic interactions between CORE pathways

As described earlier, an advantage of using this approach (deconvolution of drug MOA) to identify regulatory pathways is the possibility of discovering synergistic pathways. So in order, to explore the possible epistatic interactions between the CORE networks/ pathways, siRNAs against selected targets were combined and tested on F508del-CFTR rescue. These candidates were chosen for their potential druggability and/or strong effects on correction. Strong synergistic interactions were observed between various combinations of siRNAs against CKII, CAMKK2, MLK3 and NUP50 (a spliceosomal network component) (Figure 2G), thus validating our choice of the approach. As a note of caution here, the efficacy of the combined siRNA treatments was more variable than that observed with single siRNAs. In our experience, this is because siRNAs in combinations are less effective than the individual siRNAs in depleting their target proteins, and a depletion threshold must be reached to achieve synergy. We conclude that, using the FIT technique and a series of bioinformatic and experimental filters, we have identified a set of synergistic molecular networks that show strong control over F508del-CFTR proteostasis.

Delineation of the MLK3 and CAMKK2 signalling pathways regulating F508del-CFTR proteostasis

Next, we sought to define the composition and the role in correction of two representative CORE-networks, namely, the MLK3 and the CAMKK2 pathways. MLK3 (or MAP3K11) is part of a group of 14 MAP3 kinases that act through cascades of MAP2K and MAPK enzymes. MLK3 can be activated by various PM receptors, including the TNF-α, TGF-β, VEGF and PDGF receptors, through at least two MAP4Ks (haematopoietic progenitor kinase [HPK]1 and germinal centre kinase [GCK]) and glycogen synthase kinase (GSK)3β, or via the CDC42/Rac family [summarised in (Karen Schachter, 2006)]. MLK3 can also be activated by stress, e.g., oxidative stress (Lee et al., 2014) (i.e., it is a Stress Activated Protein Kinase, or SAPK) and it can, in turn, trigger three main kinases: p38 MAPK, c-Jun N-terminal kinase (JNK), and extracellular signal regulated kinase (ERK), depending on cell type and conditions, through the intermediate kinases MKK3/6, MKK4/7 and MKK1/2, respectively (Karen Schachter, 2006). MLK3 is also known to be an upstream activator of NF-kB (Hehner et al., 2000). We thus sought to determine which components of the MLK3 pathway have roles in F508del-CFTR correction.

The VEGF and PDGF receptors, MKK7, and NF-κB2, like MLK3, appear to be components of the correction-relevant branch of the MLK3 pathway, as indicated by the screening data in Figure 2A. Among the components upstream of MLK3, we found TGF receptors, CDC42, Rac2, and HPK1 to be active in correction (i.e. their depletion induced correction) (Figure 3A). Within the cascade downstream of MLK3, MKK7 (Figure 2A) and further downstream, JNK2 (Figure 3B) were active components (JNK2, is highly expressed in bronchial epithelial cells (http://biogps.org). The p38 MAPK, also downstream of MLK3 (through MAP2K3 and MAP2K6) was inactive in CFBE but

moderately active in HeLa cells indicating some cell-type-dependent specificity in the effects of these kinases (Figure 3-figure supplement 1A). Thus, altogether, suppression of the MKK7-JNK2 branch of the MLK3 pathway induced F508del-CFTR correction. Conversely, when the activity of the MLK3 pathway was enhanced by transfection of the MLK3 activator CDC42 or MKK7 or JNK2 into the CFBE cells, the levels of both bands B and C dropped markedly (Figure 3C), confirming that the MLK3 pathway has a tonic negative effect on the proteostasis of F508del-CFTR.

In sum, as shown in Figure 3D, a signal regulating F508del-CFTR proteostasis flows from the ligands and receptors upstream of MLK3, through HPK1 and CDC42/Rac2, to impinge on MLK3 and is then passed on through the JNK2 arm. NF-κB2 is also a probable downstream component of this proteostasis regulatory pathway. We also tested (again by siRNA silencing) seven other MAP3Ks (including TAK1/MAP3K7, see below) that can activate JNK or p38, for their effect on F508del-CFTR proteostasis. They had no effect (not shown). This highlights the remarkable specificity of MLK3 in the regulation of proteostasis, possibly due to spatial/temporal compartmentalization of the MAPK networks (Engstrom et al., 2010).

A similar series of experiments were performed to characterise the CAMKK2 cascade in F508del-CFTR correction. The results are reported in detail in Figure 3-figure supplement 1 B,C (see also Figure 3E), and indicate that the CAMKK2 pathway has negative effects on F508del-CFTR proteostasis similar to those found for the MLK3 pathway.

The MLK3 pathway exerts complex regulatory effects on F508del-CFTR proteostasis.

The increase in the levels of band B induced by inhibition of the MLK3 pathway might be due to increased synthesis or due to decreased degradation of F508del-CFTR.

Downregulation of MLK3 did not increase the CFTR mRNA levels (Figure 2- figure supplement 2B), speaking against the former possibility, though an effect of this pathway on the translational efficiency cannot be excluded. We then examined the degradation of band B using both a cycloheximide (CHX) chase and a radioactive pulse-chase assay. Downregulation of the MLK3 pathway markedly slowed the degradation of band B when measured by CHX chase assay (Figure 4A,B) and similar effects were obtained with the radioactive pulse-chase method (Figure 4- figure supplement 1A,B). We also examined the effects of enhancing the activity of MLK3 pathway by overexpressing CDC42 or MKK7 or JNK2: under these conditions the rate of degradation of band B increased 2-fold [Figure 4C,D; see also (Ferru-Clement et al., 2015)]. Notably, the ubiquitin-proteasome system itself was not detectably affected by modulation of the MLK3 pathway activity, as judged by the lack of effects on both the proteasome sensor-ZsProsensor-1 (Figure 4- figure supplement 1C) and the accumulation of poly-ubiquitinated proteins (Figure 4- figure supplement 1D). Thus, the MLK3 pathway appears to regulate the ERQC/ERAD of F508del-CFTR at a step prior to proteasomal digestion.

In addition, silencing of the MLK3 pathway (and of several CORE genes) increased also the band C/band B ratio (see Figure 2C). This is not explained by reduced ERAD alone and suggested that the MLK3 pathway might have additional effects on the folding/ export of F508del-CFTR, or on the stability of band C at the PM (or both). The trypsin susceptibility assay to assess the folding status of F508del-CFTR and an assay for protein transport out of the ER using vesicular stomatitis virus G protein (VSVG), a classical probe to study secretory trafficking, ruled out large effects of the MLK3 pathway on F508del-CFTR folding or on the general ER-export machinery (Figure 4- figure supplement 1E,F). Nevertheless, we note that these assays (trypsin susceptibility or VSVG export) are limited in their scope and do not capture the wide

spectrum of subtle regulations that can influence the outcome of proteostasis (see below for a discussion of the effect of the MLK3 pathway on folding/export). We next tested the effect of MLK3 on the stability of F508del-CFTR at the PM. We depleted MLK3 and exposed the cells to low temperature (26°C), to accumulate F508del-CFTR at the cell surface, and then shifted the cells back to 37°C, a temperature at which the F508del-CFTR at the PM is subjected to accelerated ubiquitination and degradation (Okiyoneda et al., 2010). Under these conditions, the depletion of MLK3 slowed the degradation rate of band C, increasing the $t_{1/2}$ from ~ 2 to ~ 4 h (Figure 4E,F), whereas overexpression of CDC42 to activate MLK3 enhanced the band C degradation rate (Figure 4G, H). These data suggest that also the peripheral QC of F508del-CFTR is regulated by MLK3. In contrast, the knockdown of JNK2 (or its overexpression) did not change the degradation kinetics of band C, although it increased the band C/band B ratio (not shown), suggesting that JNK2 may have additional effects, for instance on the folding and/or export of F508del-CFTR (see above and Discussion). Similar effects on F508del-CFTR folding seem likely to be induced also by many of the CORE genes whose depletion greatly increases the band C/band B ratio, in some cases up to 4-fold over control levels (Figure 2C).

In conclusion here, depletion of the receptor and stress-activated MLK3 signalling pathway markedly inhibited both the ER-associated and peripheral degradation processes of F508del-CFTR while possibly at the same time increasing the efficiency of F508del-CFTR folding/ER export. Consequently, inhibition of this pathway results in large increases in the levels of the Golgi-processed mature form of F508del-CFTR.

ROS and the CF modifiers TNF-α, TGF-β enhance F508del-CFTR degradation in an MLK3–dependent fashion.

We next examined the effects on F508del-CFTR proteostasis of agents known to activate MLK3 such as TNF-α, TGF-β (Karen Schachter, 2006) and reactive oxygen species (ROS) (Lee et al., 2014). TNF-α and TGF-β have been proposed to be genetic modifiers of CF (Cutting, 2010) and ROS have been reported to be enhanced in CF cells (Luciani et al., 2010) and to be massively produced by neutrophils during the inflammatory reactions that are common in CF patients (Witko-Sarsat et al., 1995). We treated CFBE cells with TNF-α, TGF-β or H_2O_2 (to increase ROS), and monitored the effects on F508del-CFTR. The effects of H_2O_2 at non-toxic concentrations were dramatic, with a marked drop of the F508del-CFTR levels within 30 min (Figure 5A, B). Also TNF-α and TGF-β induced rapid, though less complete (50%) decreases in levels of F508del-CFTR (Figure 5C, D). Under these conditions, the reduction in F508del-CFTR levels was completely abolished by MLK3 downregulation (Figure 5A-D), confirming the crucial role of MLK3 pathway in F508del-CFTR QC/degradation.

These results, and in particular the effects of H_2O_2, provide evidence for the existence of a rapid and potent mechanisms of protein degradation that depend on the MLK3 pathway and act on F508del-CFTR (and presumably on other misfolded mutant proteins). These regulatory mechanisms might have pathological relevance, as discussed below.

Chemical inhibitors of the MLK3 pathway act as CFTR correctors and potently synergize with the pharmacochaperone VX-809

We next tested the effect of selected kinase inhibitors on F508del-CFTR proteostasis in CFBE cells. A well-known characteristic of the kinase inhibitors is their promiscuity. In our experience, inhibitors that nominally target the same kinase can cause divergent effects on correction (see below), most likely because they target other kinases with different or competing effects. We sought to overcome this difficulty by selecting kinase

494 inhibitors with different structures and modes of action, and by using information from
495 the KINOMEscan library (http://lincs.hms.harvard.edu/data/kinomescan/). For JNK, we
496 tested a set of 10 reported JNK inhibitors (JNKi), three of which led to robust increases
497 in the levels of band B and band C (Figure 6A-D; JNKi II, JNKi IX, JNKi XI) at
498 concentrations that were required for JNK inhibition in CFBE cells (Figure 6- figure
499 supplement 1A). These JNK inhibitors have different chemical structures; moreover,
500 while JNKi II and JNKi IX are ATP-competitive inhibitors of JNK, JNKi XI is an inhibitor of
501 substrate/ scaffold binding to JNK. They therefore appear to be reliable tools to correct
502 F508del-CFTR by targeting JNK. A previously proposed MLK3 inhibitor (K252a) had no
503 clear effects on correction, perhaps because it inhibits MLK3 weakly and has diverging
504 effects on other kinases (see http://www.kinase-screen.mrc.ac.uk/screening-
505 compounds/345892). We thus searched the KINOMEscan library for a molecule that had
506 a suitable inhibitory pattern on the MLK3 pathway. (5Z)-7-oxozeaenol (hereafter referred
507 to as oxozeaenol) (Ninomiya-Tsuji et al., 2003) potently inhibits the MLK3 pathway
508 members VEGF and PDGF receptor kinases and (less potently) MLK3 itself and MKK7,
509 as well as, more weakly, a few kinases with antagonistic effects on correction
510 (http://lincs.hms.harvard.edu/db/datasets/20211/). Oxozeaenol markedly increased the
511 bands B and C of F508del-CFTR (Figure 6A-C). This drug had been identified as a
512 corrector in an earlier screening study, and proposed to have F508del-CFTR corrector
513 properties as an inhibitor of TAK1 (MAP3K7) (Trzcinska-Daneluti et al., 2012). However,
514 the downregulation of TAK1 itself had no effect on correction (Figure 6- figure
515 supplement 1B). Although the pharmacological inhibition and the siRNA knockdown of
516 kinases can sometimes have distinct consequences, these data suggest that
517 oxozeaenol likely acts through MLK3 pathway kinases to affect proteostasis rather that
518 through TAK1. In line with this notion, the corrective effects of oxozeaenol were not
519 additive with MLK3 knockdown (Figure 6- figure supplement 1C) and were accompanied

by a reduction in phospho c-jun levels (c-jun phosphorylation is diagnostic of JNK activity) (Figure 6- figure supplement 1D).

In sum, selected chemical blockers of the MLK3 (and CAMKK2; Figure 6- figure supplement 1E) pathway potently increase the levels of band B and band C as well as the band C/band B ratio (Figure 6A-D). The level of correction obtained with these inhibitors is higher than the effects of the corrector compounds from which the pathways were deduced (Figure 2- figure supplement 2A), and similar to, or higher than, the effects of VX-809.

We next considered that, while inhibitors of MLK3 pathway lead to large increases in the ER-localised band B, the pharmacochaperone VX-809 increases F508del-CFTR band C levels with only a limited effect on band B (Figure 6B-D), presumably because it primarily enhances F508del-CFTR folding. This suggested that if the large pool of band B protein accumulating in the ER following the inhibition of the MLK3 pathway is in a foldable state, VX-809 should act on such pool to enhance its folding, and greatly increase the generation of the band C mature protein. Indeed when we added both MLK3 pathway inhibitors and VX-809, there was potent synergy between them (Figure 6E,F) with increases in levels of band C that were over 20-fold the basal band C level and 4-fold over those obtained with VX-809 alone. Given the promising results of VX-809 in combination therapies in recent clinical trials (Wainwright et al., 2015) and in experimental settings (Okiyoneda et al., 2013; Phuan et al., 2014), the observed additive/ synergistic effects of VX-809 combined with MLK3 pathway inhibitors might provide a potential therapeutic opportunity.

The MLK3 pathway exerts selective effects on the proteostasis of F508del-CFTR and of structurally related mutant proteins

We next examined the effects of the MLK3 pathway inhibition on the proteostasis of other conformational disease mutants. We transfected CFBE (and HeLa) cells with different conformational mutants (i.e., Sodium-chloride symporter [NCC, R948X mutant]; P-glycoprotein, [P-gp, G268V and DY490 mutants]; human *Ether-à-go-go*-Related Gene [hERG, G601S mutant]; Wilson's disease associated protein [ATP7B, H1069Q and R778L mutants]) and then treated cells with JNKi II. The effects on their proteostasis was monitored by assessing changes in their glycosylation patterns (NCC, P-gp, hERG mutants) or in their intracellular movement from the ER to the Golgi complex (ATP7B mutants). JNKi II rescued some of these mutants (P-gp DY490 and ATP7B mutants), while it had no effects or had 'negative' effects, on others (Figure 6- figure supplement 1F). The effects on ATP7B were large and led to almost complete correction, as we report elsewhere (Chesi et al, submitted). We also tested the effect of JNKi II on other endogenous non-mutant proteins (apart from Na/K-ATPase that was a reference in many of our treatments) including, E-cadherin, IGF1R-β and EGFR (Figure 6 and Figure 6- figure supplement 1G) and found no effect on their proteostasis. Both P-glycoprotein and ATP7B, like CFTR, have two groups of transmembrane domains with an interconnecting nucleotide-binding domain. Moreover, the mutations tested (DY490 and H1069Q) are located in the nucleotide-binding domains of these proteins, and result from either a loss or substitution of aromatic amino acids, as for F508del-CFTR. These similarities suggest that a common proteostatic machinery might be involved in the processing of these mutants and can be targeted by the MLK3 pathway in a selective fashion.

DISCUSSION

In this study, we have developed a bioinformatic method based on the fuzzy intersection of drug transcriptomes (FIT) that reveals the transcriptional components of the MOAs of proteostasis correctors. Using this method, we have uncovered a set of correction-relevant genes (CORE genes), several of which belong to signalling networks that potently and selectively regulate the proteostasis of F508del-CFTR and of structurally related protein mutants.

Physio-pathological significance of the CORE signalling networks.

Based on literature data, interaction databases and our own experimental findings, the correction-relevant components we identified can be organised into five signalling cascades, which, for brevity, we refer to as the MLK3, CAMKK2, PI3K, CKII, and ERBB4 networks. Other networks were made up of constituents of the spliceosome, centromere and mediator (transcriptional) complexes, or of ubiquitin ligases.

The physiological role of these CORE signalling systems might be to regulate the stringency of the QC and degradation processes. Most of the CORE pathways enhance the efficiency of QC and degradation. This is the case of the MLK3 pathway, which can be activated by selected cytokines and by cellular stresses. The ERBB4 pathway, in contrast, is activated under growth conditions, and appears to have the effect of suppressing the QC and degradation processes. It may be speculated that cells under stress need to reduce the toxic burden of certain classes of unfolded proteins to survive, while growing cells might need to ‘tolerate’ higher levels of folding/unfolded proteins to proliferate, and that the CORE pathways regulate the proteostasis machinery according to needs. A further possibility is that at least part of the CORE pathways might function as part of an internal control system (Cancino et al., 2014; Luini et al., 2014) that is activated by the presence of unfolded/ misfolded proteins. Interestingly in this regard,

595 MLK3 interacts directly with (and might be activated by) HSP90 (Zhang et al., 2004), a
596 component of the F508del-CFTR folding and QC machinery.
597 Under pathological conditions such as cystic fibrosis and similar diseases, the
598 activity of MLK3 and other core pathways can become deleterious, as it enhances the
599 degradation of protein mutants that retain the potential to function (such as F508del-
600 CFTR). Also importantly, they can be hyper-activated under pathological conditions,
601 leading to vicious circles. For example, large amounts of ROS are produced by
602 neutrophils in the inflamed lungs of CF patients (Witko-Sarsat et al., 1995); and elevated
603 serum VEGF are detected in some CF patients (McColley et al., 2000). Both of these
604 molecules act via the MLK3 pathway to enhance the degradation of F508del-CFTR, and
605 in particular the ROS do so with striking efficacy and speed (Figure 5A,B). These effects
606 most probably result in lowering F508del-CFTR to levels below those that would be
607 determined by the primary folding defect, which might be harmful because even low
608 residual levels of F508del-CFTR may help to improve the CF phenotype in the long term
609 (Amaral, 2005). Blocking the MLK3 pathway is thus probably important to stop
610 maladaptive processes that can adversely affect therapeutic efforts. Similar
611 considerations apply to the CAMKK2 and other CORE-derived pathways.
612
613 **Mechanism of action of the MLK3 signalling network**
614 The ER quality control relies on chaperones such as HSP90 and HSC70 that are also
615 involved in folding and can switch between folding and quality control/degradation roles
616 depending on their dwell-time on the folding client proteins (Zhang et al., 2013). The
617 simplest interpretation of the data is therefore that inhibition of the MLK3 pathway
618 regulates this folding/degradation switch by impairing the entry of F508del-CFTR into the
619 degradation pathway and giving the mutant more time to fold and exit the ER. Although
620 MLK3 does not measurably affect the folding of F508del-CFTR as measured by the

621 trypsin susceptibility assay, it cannot be excluded, however, that MLK3 (and other CORE
622 genes) might exert subtle direct actions on the folding and/or ER export mechanisms.
623 This is supported by the strong effects of some of the CORE pathways on the band
624 C/band B ratio, and also by the observation that the inhibition of MLK3 markedly
625 stimulates the efficiency of export of a mutant of ATP7B (similar in structure to CFTR)
626 from the ER (Chesi et al, submitted).

627 At the molecular level, the mechanisms underlying these rescue effects remain
628 unclear. Some initial insight might come from our observation that the phosphoprotein
629 HOP co-precipitates much less efficiently with F508del-CFTR in cells treated with JNK
630 inhibitors than in control cells (Figure 4- figure supplement 1G), while its amount remains
631 unchanged. HOP serves as a link between HSC70 and HSP90 in the F508del-CFTR
632 folding process, and its depletion induces rescue of F508del-CFTR (Marozkina et al.,
633 2010), possibly by acting on the folding/ERQC switch discussed above. Thus, a reduced
634 interaction of HOP with F508del-CFTR–associated QC/folding complex might be one of
635 the possible modes of action of MLK3 on F508del-CFTR rescue. This might be an
636 example of how corrector drugs may act by modulating the 'activity', rather than the
637 levels, of relevant machinery proteins. A complete analysis of the effects of the MLK3
638 pathway on the interactions and posttranslational modifications of the ERQC/ERAD
639 machinery components remains a task for future work.

640

641 **Relevance of the CORE signalling networks for the development of clinically**
642 **useful proteostasis correctors.**

643 As already noted, this study does not aim to generate efficient correctors ready for
644 clinical use. Rather, it aims to elucidate the regulatory signalling networks that control a
645 central element of the disease *viz*. the proteostasis machinery acting on F508del-CFTR,

with a view to providing a rational basis to identify relevant pharmacological targets and, in the long run, more effective F508del-CFTR correctors.

This goal appears realistic, because signalling cascades are eminently druggable [the majority of the known drug targets are signalling components (Imming et al., 2006)], and an enormous repertoire of drugs directed at kinases and other related molecules has been developed by the pharmaceutical industry for the therapy of major diseases. For instance, over 120 inhibitors against the correction-related kinases identified in this study (not shown) are currently in clinical trial. Moreover, as shown for the case of oxozeaenol (Figure 6A-D), suitable kinase inhibitors can be selected in a rational fashion by matching the list of CORE kinases with the kinase inhibitory patterns of the many available drugs of this class, according to polypharmacology principles (Aggarwal et al., 2007). It is thus quite possible that some of these drugs may be repositioned for CF therapy. In addition, the CORE ubiquitin ligases, particularly RNF215, are also attractive targets in view of their potent effect on F508del-CFTR correction (Figure 2A). Although the technology for developing ubiquitin ligase inhibitors is still in its early stages, robust progress is being made in this direction (Goldenberg et al., 2010).

A further consideration is that the inhibitors of the CORE pathways show corrective effects that are (partially) selective for F508del-CFTR (and structurally related mutants) (see Figure 6- figure supplement 1F); and that these effects are complementary and synergic with those of the pharmacochaperone VX-809. Since these synergies lead to levels of correction that are several-fold higher than those achieved by VX-809 alone, it is possible that they result in combination therapies of clinical interest. Also of note is that the MOA-based approach used here can be exploited further in the future to identify more CORE pathways as well as more effective and specific correctors.

A remaining obstacle is the need to combine the correction of proteostasis, which is the focus of this manuscript, with the restoration of the activity of the channel. The

restitution of chloride channel conductance at the PM that we observe with the inhibitors of MLK3 pathway does not always match up to the level of rescue obtained on proteostasis alone (see also Figure 6- figure supplement 2). Notably, a similar quantitative discrepancy between the effect on proteostasis and the effect on chloride channel activity has been observed before [see (Hutt et al., 2010)]. Regulation of the chloride channel activity is a complex phenomenon and is determined by several factors including the input from signaling pathways (for e.g. PKA pathway and others), and the presence (or absence) of regulators such as NHERF and cytoskeletal components. Further studies that reveal the regulatory network controlling the activity of the channel at the PM will complement our study on proteostasis and will help in the rational design of pharmaceutical approaches.

In addition, a key requirement for translating our findings towards clinical treatments is the conservation of the CORE pathways in bronchial epithelial cells *in situ*. We have observed fundamentally similar roles of the CORE networks across several human and mammalian cell lines, both under polarized and non-polarized conditions, suggesting that these networks are well conserved. Moreover, JNK has been reported to be hyperactive in the lungs of a mice model of CF (Grassme et al., 2014), as is p38 MAPK (also activated by MLK3) in the lungs of CF patients (Berube et al., 2010) indicating that a SAPK pathway is activated under these conditions. Also notably, the MLK3 pathway inhibitor oxozeaenol has been reported to be effective in correcting the F508del-CFTR proteostasis defect in the primary human bronchial epithelial cells (Trzcinska-Daneluti et al., 2012). These observations, together with the fact that the CF genetic modifiers TNF-α and TGF-β potently affect F508del-CFTR proteostasis, support the notion that a regulatory network similar to that uncovered in CFBE cells operates on the proteostasis machinery in bronchial epithelial cells in CF patients.

In sum, this study builds on previous screening studies and on the accumulated knowledge about the F508del-CFTR proteostasis machinery (Balch et al., 2011; Farinha et al., 2013b; Lukacs and Verkman, 2012; Turnbull et al., 2007) to identify signalling pathways acting on F508del-CFTR proteostasis. This provides new insight into the physiopathology of F508del-CFTR and opens new possibilities to pharmacologically correct the folding and trafficking defect of this mutant protein. To establish the efficacy of these interventions in human bronchial epithelia and relevant animal models (Yan et al., 2015) will be the next stage towards the rational development of effective F508del-CFTR proteostasis regulators for CF patients.

MATERIALS AND METHODS

Cell culture, antibodies, plasmids and transfection

Cell lines used in this study are characterized and reported CF model systems. These include CFBE cells stably expressing wild type CFTR or F508del-CFTR (Bebok et al., 2005) and stably expressing halide sensitive YFP (Pedemonte et al., 2005) and HeLa cells stably expressing HA-tagged F508del-CFTR (Okiyoneda et al., 2010) that were obtained after material transfer agreements from the respective laboratories. These cell lines are not commercial and their STR status is unknown. Mycoplasma contamination was not observed in the cell cultures. CFBE cells were cultured in Minimal Essential Medium supplemented with 10% foetal bovine serum, non-essential amino acids, glutamine, penicillin/ streptomycin and 2 μg/ml puromycin. This media additionally supplemented with 50 μg/ml G418 was used for the CFBE-YFP cells. HeLa cells were cultured in Dulbecco's modified Eagle's medium (DMEM) supplemented with 10% foetal bovine serum, glutamine, penicillin/streptomycin and 1 μg/ml puromycin.

The antibodies used were: anti-phospho-c-jun, EGFR, IGF1R-β (Cell Signaling Technology), E-cadherin (Abcam) monoclonal anti-HA, anti-actin and anti-tubulin (Sigma), rat anti-CFTR (3G11; CFTR Folding Consortium), mouse monoclonal anti-CFTR (M3A7), HRP-conjugated anti-mouse, rabbit and rat IgG (Merckmillipore) and Anti-Na/K ATPase α1 (Thermoscientific).

The plasmids used were: JNK2 (pCDNA3 Flag MKK7B2Jnk2a2; Addgene plasmid #19727) and MKK7 (pCDNA3 Flag MKK7b1; Addgene plasmid #14622,) from Roger Davis (University of Massachusetts Medical School, Worcester, USA), ZsProSensor-1 proteasome sensor (Clontech), VSVG tagged with GFP (Jennifer Lippincott-Schwartz, NICHD, NIH, Bethesda, USA), Cdc42 (A. Hall, Sloan-Kettering Institute, New York, NY, USA), P-glycoprotein wild type, G268V and DY490 mutants

(David M. Clarke, University of Toronto, Canada) and hERG wild type and G601S mutant (Alvin Shrier, McGill University, Montreal, Canada).

The reagents used include: VX-809 (Selleckchem), JNKi II (SP600125), JNKi IX and JNKi XI (Merck Millipore), oxozeaenol (Tocris Bioscience), siRNAs (see Supplementary File 6), lipofectamine 2000 (Invitrogen) and ECL (Luminata crescendo from Merck Millipore).

Transcriptional basis of corrector MOA

To understand if the proteostatic correctors have a transcriptional component in their corrector MOA, the sensitivity of their corrector action to actinomycin D, an inhibitor of transcription, was tested. To this end, we first analysed the kinetics of action of the corrector drugs in modulating F508del-CFTR proteostasis. HeLa cells stably expressing HA-tagged F508del-CFTR (Okiyoneda et al., 2010) were treated with selected corrector drugs (from MANTRA dataset) that resulted in a detectable increase in the intensity of band B already after 3h, while the effect on band C levels were detectable only after 12-24 h of drug treatment (not shown). In order to minimize the toxic effects of actinomycin D on cell physiology and since the increase in band C was always preceded by an increase in band B, we decided to monitor the actinomycin D sensitivity of the corrector drugs towards the regulation of F508del-CFTR proteostasis by monitoring the early changes in band B levels. To this end, HeLa cells stably expressing HA-tagged F508del-CFTR were treated either with corrector drugs alone [(Chlorzoxazone (50 μM), Glafenine (50 μM), Trichostatin-A (500 nM), Dexamethasone (500 nM), Doxorubicin (500 nM)] or along with 10 ug/ml actinomycin-D for 3 h and levels of band B were determined by western blotting. While actinomycin D treatment did not have any effect on the increase in band B levels resulting from treatment with VX-325 or Corr-4a, it significantly reduced band B levels in other cases (not shown). This suggests that the corrector drugs (except

VX-325 and Corr-4a) are proteostatic regulators that act by inducing transcriptional changes in the cell.

Analysis of corrector-induced gene expression changes by microarray

Polarised CFBE41o-cells cultured at the air–liquid interface were treated with the corrector drugs of interest (CFBE dataset, Table 1) for 24hr. Total RNA was extracted and hybridization was carried out on to Whole Human Genome 44 K arrays (Agilent Technologies, product G4112A) following the manufacturer's protocol. See (Zhang et al., 2012) for experimental details. The microarray data for ouabain and low temperature treatments have been published elsewhere (Zhang et al., 2012).

FIT analysis of microarray profiles

The microarrays from the connectivity map database (https://www.broadinstitute.org/cmap/) were processed to produce prototype ranked lists (PRLs) (Iorio et al., 2010). In these PRLs, cell line specific responses are diluted, thus summarising consensual transcriptional responses to drug treatment. In each PRL, microarray probe-sets are ordered from the most upregulated to most downregulated one. We downloaded PRLs for the whole panel of small molecules in the connectivity map (www.connectivitymap.org) from which the MANTRA database is derived (http://mantra.tigem.it/). We used these in conjunction with ranked lists of probe sets based on fold-changes [and assembled following the guidelines provided in (Iorio et al., 2010)] from microarray profiles that we generated in house (CFBE dataset).

The FIT analysis identifies microarray probe-sets that tend to respond consistently to a group of drugs [see also (Iorio et al., 2010) for description of a similar method]. The top and bottom 20% of the probe-sets (corresponding to the up- and downregulated probe-sets respectively) were used for the analysis. The 20% cut-off was

used since the merging of individual gene expression profiles into PRLs precludes the application of other thresholds based on fold-change (or p-value) to identify significantly differentially expressed genes. To build a null model against which the significance of the final genes sets can be tested (as detailed below), a fixed number of PRLs (N) from the MANTRA dataset were randomly selected and the upregulated or downregulated probe-sets from this selection were intersected by varying the fuzzy cut-off threshold (i.e. the ratio of drugs that a given probe-set should transcriptionally respond to, in order to be considered 'consistently' regulated, hence to be included in the fuzzy intersection). After 1000 of these iterations, we derived an empirical null distribution of the number of probes included in the resulting fuzzy intersections and used it for p-value assignments (Figure 1B). For the CFBE dataset, (generated on an Agilent platform, which is different from that used for the connectivity map and MANTRA database) we derived this null distribution by randomly permuting all the individual probes. Finally, we determined the optimal fuzzy cut-off values for the transcriptional profiles elicited by the corrector drugs (11 contained in MANTRA and 13 in the CFBE dataset). Briefly, we selected the value such that the number of probes present in the final fuzzy intersection was at least 3 fold higher than that expected by random chance and its p-value < 0.05 (according to the computed null models). By using this method, no significantly upregulated probes from the MANTRA dataset were identified across all of the range of tested fuzzy cut-offs. For the downregulated probe-sets a fuzzy cut-off of 8 (out of 11 corrector drugs) or above produced significant fuzzy intersection of probe-sets. For the CFBE dataset, a significant cut-off of 6 drugs (out of 13) and above was identified. To further optimise the selection of these cut-offs, we chose the maximal cut-off yielding a fuzzy intersection of probe-sets enriched in one or more Gene Ontology terms. With this criterion, we obtained a final cut-off value of 8 for the MANTRA down-regulated probe set and cut-off of 9 for the CFBE dataset. Intersecting the corrector-induced gene expression profiles using this

optimal fuzzy cut-off resulted in 541 upregulated probe-sets (mapping 402 unique genes) and 191 downregulated probe-sets (mapping to 117 unique genes) for the CFBE dataset, and 108 downregulated probe-sets (mapping 102 genes) for the MANTRA dataset. Note, that most of the CORE genes (519 out of the 621 CORE genes) are derived from the CFBE dataset. This we suppose is due to the use of PRLs in the case of cMAP dataset and use of data derived from a single cell line in the case of CFBE dataset. The use of single cell line derived data can potentially lead to high number of false positives since perturbation-independent response of cell lines to treatments is usually stronger than the perturbation-dependent response (Iorio et al., 2010).

We finally validated the optimal number of drugs that need to be considered for a fuzzy cut-off of 70% (corresponding to 8 out 11 drugs cut-off from the MANTRA dataset), providing a minimum number of false positives in the intersection (i.e. genes expected to be contained in the resulting intersections by random chance). This was performed by a permutation test where, in a series of iterations, the fuzzy cut-off is kept constant and the number of randomly selected drugs varied within a given range (specifically from 1 to 20). At each of these iterations we computed the cardinality of the resulting fuzzy intersections, observing that this value reached a plateau at 10 drugs (Figure 1C), which suggests that the number of drugs that was used in the analysis (i.e. 11 drugs in the cMAP dataset) was fairly close to the optimal level.

Protein-protein interaction

The protein-protein interactions were downloaded from the STRING database (http://string-db.org/) (Franceschini et al., 2013), and those with a confidence level of >0.7 were used for the analysis. To build the proteostasis gene (PG) dataset, we included known proteostatic regulators of CFTR i.e., proteins where their expression/ activity level changes have been shown to affect CFTR proteostasis. We also included

836 the interactors of CFTR and CF pathology related genes/ proteins present in GeneGO
837 Metaminer Cystic Fibrosis database (see Supplementary File 4 for the list of the
838 proteostasis genes). The number of interactions observed among the CORE gene
839 dataset and the proteostasis gene dataset as well as among the CORE gene dataset
840 were more than expected on a random basis and were statistically significant. For details
841 on the statistical test used see (Franceschini et al., 2013).
842
843 **Ingenuity pathway analysis (IPA)**
844 The gene sets were analyzed using the CORE analysis application of the Ingenuity
845 pathway analysis, a web-based software application. The default settings of the analysis
846 were used. Each network had an assigned significance score based on the *p*-value
847 (calculated using Fischer‘s exact test) for the probability of finding the focus genes in a
848 set of genes randomly selected from the global molecular network. The upregulated and
849 downregulated genes of the CFBE dataset and the downregulated genes of the cMAP
850 dataset were analyzed separately and also together, to infer common pathways or
851 networks embedded among them.
852
853 **Cell lysis, western blotting and analysis**
854 Cells were washed three times in ice-cold Dulbecco’s phosphate-buffered saline, and
855 lysed in RIPA buffer (150 mM NaCl, 1% Triton X-100, 0.5% deoxycholic acid, 0.1% SDS,
856 20 mM Tris-HCl, pH 7.4), supplemented with protease inhibitor cocktail and phosphatase
857 inhibitors. The lysates were clarified by centrifugation at 15000 x g for 15 min, and the
858 supernatants were resolved by SDS-PAGE. BCA Protein Assay kit (Pierce) was used to
859 quantitate protein levels before loading. The western blots were developed with
860 appropriate antibodies and using ECL. The blots were then exposed to x-ray films and
861 exposure time was varied to obtain optimal signal. The x-ray films were then scanned

and the bands were quantitated using ImageJ gel-analysis tool (see Figure 2- figure supplement 2A-D). The protein concentration and the exposures used for quantitation of the blots were optimized to be in a linear range of detection (Figure 2- figure supplement 1E,F).

Biochemical screening assay:

Each gene was targeted by 3 siRNAs and as control non-targeting siRNAs provided by the manufacturer were used (see Supplementary File 6 for list of siRNAs used). A gene was considered as active if: (1) at least two different siRNAs targeting a gene gave concordant changes in the levels of band C that was >2 SD from the mean value of the control siRNAs and (2) the change in band C levels was ±20% of the level of band C obtained with the control siRNAs. Those genes that increased band C levels significantly upon their downregulation were termed anti-correction genes and those that decreased band C levels were termed pro-correction genes.

A potential problem in siRNA-based experiments is the possibility of off-target effects. The specificity of the observed effects on F508del-CFTR proteostasis are supported by the following lines of evidence: **1)** The quantitation of the on-target effect of the siRNAs by RT-PCR (see Figure 2- figure supplement 3) which shows that treatment with siRNAs brings down the transcript levels of the target genes to about 10-30% of the levels present in cells treated with non-targeting siRNAs. **2)** The use of at least 3 different siRNAs (individually) for the screenings, majority of which showed concordant results on proteostasis. Moreover, for selected genes (MLK3, CAMKK2, RNF215, NUP50 and CD2BP2), the findings from the screening studies were reinforced using additional siRNAs (for instance, 5 additional siRNAs for MLK3; see Supplementary File 6 for details of the siRNAs used) that showed similar effects on proteostasis of F508del-CFTR (not shown). **3)** The coherent effects of the siRNA targeting different genes of signaling pathways supports the functional significance of the effects of each siRNA (see

Figure 3A,B and Figure 3- figure supplement 1B) **4)** Overexpression of identified hits show an opposite effect on proteostasis to that of the siRNAs (see below Figure 3C), **5)** Finally, there was a positive correlation between the concentration of siRNAs used and the effect on proteostasis (Figure 2- figure supplement 3). All these evidences together confirm the specificity of the observed effect of the siRNAs on proteostasis.

Immunoprecipitation

HeLa cells cultured in 10-cm plates (80% confluence) were treated with appropriate corrector drugs for 24h. The cells then were washed three times in ice-cold Dulbecco's phosphate-buffered saline, and lysed in immunoprecipitation buffer (150 mM NaCl, 1% Triton X-100, 20 mM Tris-HCl, pH 7.4) on ice for 30min. The lysates were clarified by centrifugation at 15000 x g for 15 min, and the protein content of the supernatants quantitated by BCA Protein Assay kit (Pierce). Equal amounts of proteins from control and treated cell lysates were incubated with Protein-G sepharose beads conjugated with anti-HA antibody (Sigma) overnight at 4 °C. The beads were then washed in the immunoprecipitation buffer 5 times and the bound proteins eluted with HA-peptide (Sigma) at a concentration of 100 µg/ml. The eluted proteins were then resolved by SDS-PAGE and then immunoblotted.

Partial trypsin digestion of CFTR

The trypsin digestion assay was similar to that described previously (Zhang et al., 1998). Cells were grown in a 10-cm plate and post-treatment they were washed three times with 10 mL phosphate-buffered saline (PBS). They were then scraped in 5 ml PBS, and pelleted at 500 x g for 5 min in 4 °C. The cell pellet was resuspended in 1 mL of hypertonic buffer (250 mM sucrose, 10 mM Hepes, pH 7.2) and the cells were then homogenized using a ball bearing homogenizer. The nuclei and unbroken cells were

914 removed by centrifugation at 600 x *g* for 15 min. The membranes were then pelleted by
915 centrifugation at 100000 x *g* for 30 min, and then resuspended in digestion buffer (40
916 mM Tris pH 7.4, 2 mM $MgCl_2$, 0.1 mM EDTA). Then membranes corresponding to 50 µg
917 of protein were incubated with different concentrations of trypsin (1 to 50 µg/ml) on ice
918 for 15 min. The reactions were stopped with the addition of soya bean trypsin inhibitor
919 (Sigma) to a final concentration of 1 mM, and the samples were immediately denatured
920 in sample buffer (62.5 mM Tris-HCL, pH 6.8, 2% SDS, 10% glycerol, 0.001%
921 bromophenol, 125 mM dithiothreitol) at 37 °C for 30 min. The samples were resolved on
922 4% to 16% gradient SDS-PAGE (Tris-glycine) and transferred onto nitrocellulose
923 membranes. These membranes were developed with the 3G11 anti-CFTR antibodies
924 (that recognize nucleotide-binding domain 1 - NBD1) or the M3A7 clone (that recognizes
925 nucleotide-binding domain 2 -NBD2).
926
927 **Plasma membrane quality control assay**
928 The PQC assay was essentially as described previously (Okiyoneda et al., 2010). CFBE
929 cells were untreated or treated with siRNAs for 72 h and for the final 31 h they were kept
930 at low temperature (26 °C) and for an additional 5 h at 26 °C with CHX (100 µg/ml).
931 Then the cells were shifted to 37 °C for 1.5 h with 100 µg/ml CHX before the turnover
932 measurements started at 37 °C. The cells were lysed at 0, 1, 3 and 5 h and the kinetics
933 of degradation of band C was examined by immunoblotting.
934
935 **Halide sensitive YFP assay for CFTR activity**
936 Twenty-four hours after plating, the CFBE cells that stably expressed halide sensitive
937 YFP were incubated with the test compounds at 37 °C for 48 h. At the time of the assay,
938 the cells were washed with PBS (containing 137 mM NaCl, 2.7 mM KCl, 8.1 mM
939 Na_2HPO_4, 1.5 mM KH_2PO_4, 1 mM $CaCl_2$, 0.5 mM $MgCl_2$) and stimulated for 30 min with

20 µm forskolin and 50 µm genistein. The cells were then transferred to a Zeiss LSM700 confocal microscope, where the images were acquired with a 20x objective (0.50 NA) and with an open pinhole (459 µm) at a rate of 330 ms/frame (each frame corresponding to 159.42 µm x 159.42 µm), at ambient temperature. The excitation laser line 488nm was used at 2% efficiency coupled to a dual beam splitter (621nm) for detection. The images (8-bit) were acquired in a 512x512 format with no averaging to maximize the speed of acquisition. Each assay consisted of a continuous 300-s fluorescence reading with 30 s before and the rest after injection of an iodide-containing solution (PBS with Cl^- replaced by I^-; final I^- concentration in the well, 100 mM). To determine the fluorescence-quenching rate associated with I^- influx, the final 200 s of the data for each well were fitted with a mono-exponential decay, and the decay constant K was calculated using GraphPad Prism software.

Ussing chamber assay for short circuit current recordings

Short-circuit current (I_{sc}) was measured across monolayers in modified Ussing chambers. CFBE41o$^-$ cells ($1x10^6$) were seeded onto 12-mm fibronectin-coated Snapwell inserts (Corning Incorporated) and the apical medium was removed after 24h to establish an air-liquid interface. Transepithelial resistance was monitored using an EVOM epithelial volt-ohmmeter and cells were used when the transepithelial resistance was 300-400 $\Omega.cm^2$. CFBE41o$^-$ monolayers were treated on both sides with optiMEM medium containing 2% (v/v) FBS and one of the following compound: 0.1% DMSO (negative control), or compounds at the stated dosage for 48h before being mounted in EasyMount chambers and voltage clamped using a VCCMC6 multichannel current-voltage clamp (Physiologic Instruments). The apical membrane conductance was functionally isolated by permeabilising the basolateral membrane with 200µg/ml nystatin and imposing an apical-to-basolateral Cl^- gradient. The basolateral bathing solution contained 1.2 mM

NaCl, 115 mM Na-gluconate, 25 mM $NaHCO_3$, 1.2 mM $MgCl_2$, 4 mM $CaCl_2$, 2.4 mM KH_2PO_4, 1.24 mM K_2HPO_4 and 10 mM glucose (pH 7.4). The $CaCl_2$ concentration was increased to 4mM to compensate for the chelation of calcium by gluconate. The apical bathing solution contained 115 mM NaCl, 25 mM $NaHCO_3$, 1.2 mM $MgCl_2$, 1.2 mM $CaCl_2$, 2.4 mM KH_2PO_4, 1.24 mM K_2HPO_4 and 10 mM mannitol (pH 7.4). The apical solution contained mannitol instead of glucose to eliminate currents mediated by Na^+-glucose co-transport. Successful permeabilization of the basolateral membrane was obvious from the reversal of I_{sc} under these conditions. Solutions were continuously gassed and stirred with 95% O_2-5% CO_2 and maintained at 37°C. Ag/AgCl reference electrodes were used to measure transepithelial voltage and pass current. Pulses (1mV amplitude, 1s duration) were delivered every 90s to monitor resistance. The voltage clamps were connected to a PowerLab/8SP interface for data collection. CFTR was activated by adding 10 μM forskolin to the apical bathing solution.

SUPPLEMENTARY FILES:

Supplementary File 1: The microarray data for the CFBE dataset (related to Figure 1).

Supplementary File 2: Drug communities containing the 11 MANTRA drugs extracted from the MANTRA drug similarity network assembled in (Iorio et al., 2010) (related to Figure 1- figure supplement 1).

Supplementary File 3: The CORE genes obtained using the FIT analysis and list of genes selected for experimental validation (related to Figures 1 and 2).

Supplementary File 4: The proteostasis genes used for this study (related to Figure 1).

Supplementary File 5: The regulatory and proteostasis genes present in the CORE genes list (related to Figure 1).

Supplementary File 6: The siRNAs used in this study (related to Figure 2).

Author Contributions: RNH, SP, AL designed and developed the idea and wrote the manuscript. RNH, SP, AS and LB conducted the experiments largely at IBP, CNR. FCi and DYT produced the microarray data in CFBE41o- cells. AC, DC, FCi, DdB were involved in microarray data analysis. FCi, FI, FCa, VB, MP, and DdB were involved in the bio-informatics analysis. GC and LG helped in the anion conductance assays.

ACKNOWLEDGEMENTS:

We acknowledge the financial support of Italian Cystic Fibrosis Research Foundation (FFC#2 2014), Fondazione Telethon, AIRC (Italian Association for Cancer Research, IG 10593), the MIUR Project “FaReBio di Qualità”, the PON projects no. 01/00117 and 01-00862, PONa3-00025 (BIOforIU), PNR-CNR Aging Program 2012-2014 and Progetto Bandiera 'Epigen' to AL, Fondazione Telethon and Ministero della Salute, Italy to DdB. FCi was supported by a postdoctoral fellowship from Pasteur Institute Cenci-Bolognetti Foundation, Biology and Biotechnology Department "Charles Darwin" of Sapienza University of Rome, and partially funded by the Telethon Institute of genetics and Medicine. GC was supported by a fellowship from Cystic Fibrosis Canada and by the Canadian Institutes for Health Research. DYT is the Canada Research Chair in Molecular Genetics. DYT acknowledges the support from Canada Foundation for Innovation and the Canadian Institutes for Health Research (MOP-89779). We thank the Bioinformatic core Facility of the Telethon Institute of Genetics and Medicine, for help with bioinformatics analysis and the Bioimaging Facility of the Institute of Protein Biochemistry for help with the image acquisition.

REFERENCES:

Aggarwal, B.B., G. Sethi, V. Baladandayuthapani, S. Krishnan, and S. Shishodia. 2007. Targeting cell signaling pathways for drug discovery: an old lock needs a new key. *J Cell Biochem*. 102:580-592.

Amaral, M.D. 2005. Processing of CFTR: traversing the cellular maze--how much CFTR needs to go through to avoid cystic fibrosis? *Pediatric pulmonology*. 39:479-491.

Anjos, S.M., R. Robert, D. Waller, D.L. Zhang, H. Balghi, H.M. Sampson, F. Ciciriello, P. Lesimple, G.W. Carlile, J. Goepp, J. Liao, P. Ferraro, R. Phillipe, F. Dantzer, J.W. Hanrahan, and D.Y. Thomas. 2012. Decreasing Poly(ADP-Ribose) Polymerase Activity Restores DeltaF508 CFTR Trafficking. *Front Pharmacol*. 3:165.

Balch, W.E., D.M. Roth, and D.M. Hutt. 2011. Emergent properties of proteostasis in managing cystic fibrosis. *Cold Spring Harb Perspect Biol*. 3.

Bebok, Z., J.F. Collawn, J. Wakefield, W. Parker, Y. Li, K. Varga, E.J. Sorscher, and J.P. Clancy. 2005. Failure of cAMP agonists to activate rescued deltaF508 CFTR in CFBE41o- airway epithelial monolayers. *J Physiol*. 569:601-615.

Berube, J., L. Roussel, L. Nattagh, and S. Rousseau. 2010. Loss of cystic fibrosis transmembrane conductance regulator function enhances activation of p38 and ERK MAPKs, increasing interleukin-6 synthesis in airway epithelial cells exposed to Pseudomonas aeruginosa. *J Biol Chem*. 285:22299-22307.

Calamini, B., M.C. Silva, F. Madoux, D.M. Hutt, S. Khanna, M.A. Chalfant, S.A. Saldanha, P. Hodder, B.D. Tait, D. Garza, W.E. Balch, and R.I. Morimoto. 2012. Small-molecule proteostasis regulators for protein conformational diseases. *Nat Chem Biol*. 8:185-196.

Cancino, J., A. Capalbo, A. Di Campli, M. Giannotta, R. Rizzo, J.E. Jung, R. Di Martino, M. Persico, P. Heinklein, M. Sallese, and A. Luini. 2014. Control systems of membrane transport at the interface between the endoplasmic reticulum and the Golgi. *Developmental cell*. 30:280-294.

Caohuy, H., C. Jozwik, and H.B. Pollard. 2009. Rescue of DeltaF508-CFTR by the SGK1/Nedd4-2 signaling pathway. *J Biol Chem*. 284:25241-25253.

Carlile, G.W., R.A. Keyzers, K.A. Teske, R. Robert, D.E. Williams, R.G. Linington, C.A. Gray, R.M. Centko, L. Yan, S.M. Anjos, H.M. Sampson, D. Zhang, J. Liao, J.W. Hanrahan, R.J. Andersen, and D.Y. Thomas. 2012. Correction of F508del-CFTR trafficking by the sponge alkaloid latonduine is modulated by interaction with PARP. *Chem Biol*. 19:1288-1299.

Chia, J., G. Goh, V. Racine, S. Ng, P. Kumar, and F. Bard. 2012. RNAi screening reveals a large signaling network controlling the Golgi apparatus in human cells. *Molecular systems biology*. 8:629.

Cutting, G.R. 2010. Modifier genes in Mendelian disorders: the example of cystic fibrosis. *Ann N Y Acad Sci*. 1214:57-69.

De Matteis, M.A., G. Santini, R.A. Kahn, G. Di Tullio, and A. Luini. 1993. Receptor and protein kinase C-mediated regulation of ARF binding to the Golgi complex. *Nature*. 364:818-821.

Engstrom, W., A. Ward, and K. Moorwood. 2010. The role of scaffold proteins in JNK signalling. *Cell proliferation*. 43:56-66.

Farhan, H., M.W. Wendeler, S. Mitrovic, E. Fava, Y. Silberberg, R. Sharan, M. Zerial, and H.P. Hauri. 2010. MAPK signaling to the early secretory pathway revealed by kinase/phosphatase functional screening. *J Cell Biol*. 189:997-1011.

Farinha, C.M., J. King-Underwood, M. Sousa, A.R. Correia, B.J. Henriques, M. Roxo-Rosa, A.C. Da Paula, J. Williams, S. Hirst, C.M. Gomes, and M.D. Amaral. 2013a. Revertants, low temperature, and correctors reveal the mechanism of F508del-CFTR rescue by VX-809 and suggest multiple agents for full correction. *Chem Biol*. 20:943-955.

Farinha, C.M., P. Matos, and M.D. Amaral. 2013b. Control of cystic fibrosis transmembrane conductance regulator membrane trafficking: not just from the endoplasmic reticulum to the Golgi. *Febs J*. 280:4396-4406.

Ferru-Clement, R., F. Fresquet, C. Norez, T. Metaye, F. Becq, A. Kitzis, and V. Thoreau. 2015. Involvement of the Cdc42 Pathway in CFTR Post-Translational Turnover and in Its Plasma Membrane Stability in Airway Epithelial Cells. *PLoS One*. 10:e0118943.

Franceschini, A., D. Szklarczyk, S. Frankild, M. Kuhn, M. Simonovic, A. Roth, J. Lin, P. Minguez, P. Bork, C. von Mering, and L.J. Jensen. 2013. STRING v9.1: protein-protein interaction networks, with increased coverage and integration. *Nucleic Acids Res*. 41:D808-815.

Gentzsch, M., X.B. Chang, L. Cui, Y. Wu, V.V. Ozols, A. Choudhury, R.E. Pagano, and J.R. Riordan. 2004. Endocytic trafficking routes of wild type and DeltaF508 cystic fibrosis transmembrane conductance regulator. *Mol Biol Cell*. 15:2684-2696.

Giannotta, M., C. Ruggiero, M. Grossi, J. Cancino, M. Capitani, T. Pulvirenti, G.M. Consoli, C. Geraci, F. Fanelli, A. Luini, and M. Sallese. 2012. The KDEL receptor couples to Galphaq/11 to activate Src kinases and regulate transport through the Golgi. *The EMBO journal*. 31:2869-2881.

Goldenberg, S.J., J.G. Marblestone, M.R. Mattern, and B. Nicholson. 2010. Strategies for the identification of ubiquitin ligase inhibitors. *Biochemical Society transactions*. 38:132-136.

Grassme, H., A. Carpinteiro, M.J. Edwards, E. Gulbins, and K.A. Becker. 2014. Regulation of the inflammasome by ceramide in cystic fibrosis lungs. *Cell Physiol Biochem*. 34:45-55.

Hart, Y., and U. Alon. 2013. The utility of paradoxical components in biological circuits. *Mol Cell*. 49:213-221.

Hehner, S.P., T.G. Hofmann, A. Ushmorov, O. Dienz, I. Wing-Lan Leung, N. Lassam, C. Scheidereit, W. Droge, and M.L. Schmitz. 2000. Mixed-lineage kinase 3 delivers CD3/CD28-derived signals into the IkappaB kinase complex. *Mol Cell Biol*. 20:2556-2568.

Hutt, D.M., D. Herman, A.P. Rodrigues, S. Noel, J.M. Pilewski, J. Matteson, B. Hoch, W. Kellner, J.W. Kelly, A. Schmidt, P.J. Thomas, Y. Matsumura, W.R. Skach, M. Gentzsch, J.R. Riordan, E.J. Sorscher, T. Okiyoneda, J.R. Yates, 3rd, G.L. Lukacs, R.A. Frizzell, G. Manning, J.M. Gottesfeld, and W.E. Balch. 2010. Reduced histone deacetylase 7 activity restores function to misfolded CFTR in cystic fibrosis. *Nat Chem Biol*. 6:25-33.

1105 Imming, P., C. Sinning, and A. Meyer. 2006. Drugs, their targets and the nature and
1106 number of drug targets. *Nat Rev Drug Discov*. 5:821-834.
1107 Iorio, F., R. Bosotti, E. Scacheri, V. Belcastro, P. Mithbaokar, R. Ferriero, L. Murino, R.
1108 Tagliaferri, N. Brunetti-Pierri, A. Isacchi, and D. di Bernardo. 2010. Discovery of
1109 drug mode of action and drug repositioning from transcriptional responses. *Proc*
1110 *Natl Acad Sci U S A*. 107:14621-14626.
1111 Iskar, M., G. Zeller, P. Blattmann, M. Campillos, M. Kuhn, K.H. Kaminska, H. Runz,
1112 A.C. Gavin, R. Pepperkok, V. van Noort, and P. Bork. 2013. Characterization of
1113 drug-induced transcriptional modules: towards drug repositioning and functional
1114 understanding. *Molecular systems biology*. 9:662.
1115 Jensen, T.J., M.A. Loo, S. Pind, D.B. Williams, A.L. Goldberg, and J.R. Riordan. 1995.
1116 Multiple proteolytic systems, including the proteasome, contribute to CFTR
1117 processing. *Cell*. 83:129-135.
1118 Kalid, O., M. Mense, S. Fischman, A. Shitrit, H. Bihler, E. Ben-Zeev, N. Schutz, N.
1119 Pedemonte, P.J. Thomas, R.J. Bridges, D.R. Wetmore, Y. Marantz, and H.
1120 Senderowitz. 2010. Small molecule correctors of F508del-CFTR discovered by
1121 structure-based virtual screening. *J Comput Aided Mol Des*. 24:971-991.
1122 Karen Schachter, G.-Y.L., Yan Du, Kathleen A Gallo. 2006. MLK3. *UCSD Nature*
1123 *Molecule Pages*.
1124 Kunzelmann, K., E.M. Schwiebert, P.L. Zeitlin, W.L. Kuo, B.A. Stanton, and D.C.
1125 Gruenert. 1993. An immortalized cystic fibrosis tracheal epithelial cell line
1126 homozygous for the delta F508 CFTR mutation. *American journal of respiratory*
1127 *cell and molecular biology*. 8:522-529.
1128 Lee, H.S., C.Y. Hwang, S.Y. Shin, K.S. Kwon, and K.H. Cho. 2014. MLK3 is part of a
1129 feedback mechanism that regulates different cellular responses to reactive oxygen
1130 species. *Science signaling*. 7:ra52.
1131 Loo, M.A., T.J. Jensen, L. Cui, Y. Hou, X.B. Chang, and J.R. Riordan. 1998.
1132 Perturbation of Hsp90 interaction with nascent CFTR prevents its maturation and
1133 accelerates its degradation by the proteasome. *The EMBO journal*. 17:6879-6887.
1134 Lu, J.J., W. Pan, Y.J. Hu, and Y.T. Wang. 2012. Multi-target drugs: the trend of drug
1135 research and development. *PLoS One*. 7:e40262.
1136 Luciani, A., V.R. Villella, S. Esposito, N. Brunetti-Pierri, D. Medina, C. Settembre, M.
1137 Gavina, L. Pulze, I. Giardino, M. Pettoello-Mantovani, M. D'Apolito, S. Guido, E.
1138 Masliah, B. Spencer, S. Quaratino, V. Raia, A. Ballabio, and L. Maiuri. 2010.
1139 Defective CFTR induces aggresome formation and lung inflammation in cystic
1140 fibrosis through ROS-mediated autophagy inhibition. *Nat Cell Biol*. 12:863-875.
1141 Luini, A., G. Mavelli, J. Jung, and J. Cancino. 2014. Control systems and coordination
1142 protocols of the secretory pathway. *F1000prime reports*. 6:88.
1143 Lukacs, G.L., and A.S. Verkman. 2012. CFTR: folding, misfolding and correcting the
1144 DeltaF508 conformational defect. *Trends Mol Med*. 18:81-91.
1145 Marozkina, N.V., S. Yemen, M. Borowitz, L. Liu, M. Plapp, F. Sun, R. Islam, P.
1146 Erdmann-Gilmore, R.R. Townsend, C.F. Lichti, S. Mantri, P.W. Clapp, S.H.
1147 Randell, B. Gaston, and K. Zaman. 2010. Hsp 70/Hsp 90 organizing protein as a
1148 nitrosylation target in cystic fibrosis therapy. *Proc Natl Acad Sci U S A*.
1149 107:11393-11398.

McColley, S.A., V. Stellmach, S.R. Boas, M. Jain, and S.E. Crawford. 2000. Serum vascular endothelial growth factor is elevated in cystic fibrosis and decreases with treatment of acute pulmonary exacerbation. *Am J Respir Crit Care Med*. 161:1877-1880.

Meacham, G.C., Z. Lu, S. King, E. Sorscher, A. Tousson, and D.M. Cyr. 1999. The Hdj-2/Hsc70 chaperone pair facilitates early steps in CFTR biogenesis. *The EMBO journal*. 18:1492-1505.

Ninomiya-Tsuji, J., T. Kajino, K. Ono, T. Ohtomo, M. Matsumoto, M. Shiina, M. Mihara, M. Tsuchiya, and K. Matsumoto. 2003. A resorcylic acid lactone, 5Z-7-oxozeaenol, prevents inflammation by inhibiting the catalytic activity of TAK1 MAPK kinase kinase. *J Biol Chem*. 278:18485-18490.

Odolczyk, N., J. Fritsch, C. Norez, N. Servel, M.F. da Cunha, S. Bitam, A. Kupniewska, L. Wiszniewski, J. Colas, K. Tarnowski, D. Tondelier, A. Roldan, E.L. Saussereau, P. Melin-Heschel, G. Wieczorek, G.L. Lukacs, M. Dadlez, G. Faure, H. Herrmann, M. Ollero, F. Becq, P. Zielenkiewicz, and A. Edelman. 2013. Discovery of novel potent DeltaF508-CFTR correctors that target the nucleotide binding domain. *EMBO molecular medicine*. 5:1484-1501.

Okiyoneda, T., H. Barriere, M. Bagdany, W.M. Rabeh, K. Du, J. Hohfeld, J.C. Young, and G.L. Lukacs. 2010. Peripheral protein quality control removes unfolded CFTR from the plasma membrane. *Science*. 329:805-810.

Okiyoneda, T., G. Veit, J.F. Dekkers, M. Bagdany, N. Soya, H. Xu, A. Roldan, A.S. Verkman, M. Kurth, A. Simon, T. Hegedus, J.M. Beekman, and G.L. Lukacs. 2013. Mechanism-based corrector combination restores DeltaF508-CFTR folding and function. *Nat Chem Biol*. 9:444-454.

Pedemonte, N., G.L. Lukacs, K. Du, E. Caci, O. Zegarra-Moran, L.J. Galietta, and A.S. Verkman. 2005. Small-molecule correctors of defective DeltaF508-CFTR cellular processing identified by high-throughput screening. *J Clin Invest*. 115:2564-2571.

Phuan, P.W., G. Veit, J. Tan, A. Roldan, W.E. Finkbeiner, G.L. Lukacs, and A.S. Verkman. 2014. Synergy-based Small-Molecule Screen Using a Human Lung Epithelial Cell Line Yields DeltaF508-CFTR Correctors that Augment VX-809 Maximal Efficacy. *Mol Pharmacol*.

Popescu, F.D. 2003. New asthma drugs acting on gene expression. *J Cell Mol Med*. 7:475-486.

Pulvirenti, T., M. Giannotta, M. Capestrano, M. Capitani, A. Pisanu, R.S. Polishchuk, E. San Pietro, G.V. Beznoussenko, A.A. Mironov, G. Turacchio, V.W. Hsu, M. Sallese, and A. Luini. 2008. A traffic-activated Golgi-based signalling circuit coordinates the secretory pathway. *Nat Cell Biol*. 10:912-922.

Riordan, J.R. 2008. CFTR function and prospects for therapy. *Annu Rev Biochem*. 77:701-726.

Rosser, M.F., D.E. Grove, L. Chen, and D.M. Cyr. 2008. Assembly and misassembly of cystic fibrosis transmembrane conductance regulator: folding defects caused by deletion of F508 occur before and after the calnexin-dependent association of membrane spanning domain (MSD) 1 and MSD2. *Mol Biol Cell*. 19:4570-4579.

Roth, D.M., D.M. Hutt, J. Tong, M. Bouchecareilh, N. Wang, T. Seeley, J.F. Dekkers, J.M. Beekman, D. Garza, L. Drew, E. Masliah, R.I. Morimoto, and W.E. Balch.

2014. Modulation of the maladaptive stress response to manage diseases of protein folding. *PLoS biology*. 12:e1001998.

Ryno, L.M., R.L. Wiseman, and J.W. Kelly. 2013. Targeting unfolded protein response signaling pathways to ameliorate protein misfolding diseases. *Current opinion in chemical biology*. 17:346-352.

Sampson, H.M., R. Robert, J. Liao, E. Matthes, G.W. Carlile, J.W. Hanrahan, and D.Y. Thomas. 2011. Identification of a NBD1-binding pharmacological chaperone that corrects the trafficking defect of F508del-CFTR. *Chem Biol*. 18:231-242.

Santagata, S., M.L. Mendillo, Y.C. Tang, A. Subramanian, C.C. Perley, S.P. Roche, B. Wong, R. Narayan, H. Kwon, M. Koeva, A. Amon, T.R. Golub, J.A. Porco, Jr., L. Whitesell, and S. Lindquist. 2013. Tight coordination of protein translation and HSF1 activation supports the anabolic malignant state. *Science*. 341:1238303.

Simpson, J.C., B. Joggerst, V. Laketa, F. Verissimo, C. Cetin, H. Erfle, M.G. Bexiga, V.R. Singan, J.K. Heriche, B. Neumann, A. Mateos, J. Blake, S. Bechtel, V. Benes, S. Wiemann, J. Ellenberg, and R. Pepperkok. 2012. Genome-wide RNAi screening identifies human proteins with a regulatory function in the early secretory pathway. *Nat Cell Biol*. 14:764-774.

Trzcinska-Daneluti, A.M., A. Chen, L. Nguyen, R. Murchie, C. Jiang, J. Moffat, L. Pelletier, and D. Rotin. 2015. RNA Interference Screen to Identify Kinases That Suppress Rescue of DeltaF508-CFTR. *Mol Cell Proteomics*. 14:1569-1583.

Trzcinska-Daneluti, A.M., L. Nguyen, C. Jiang, C. Fladd, D. Uehling, M. Prakesch, R. Al-awar, and D. Rotin. 2012. Use of kinase inhibitors to correct DeltaF508-CFTR function. *Mol Cell Proteomics*. 11:745-757.

Turnbull, E.L., M.F. Rosser, and D.M. Cyr. 2007. The role of the UPS in cystic fibrosis. *BMC biochemistry*. 8 Suppl 1:S11.

Van Goor, F., K.S. Straley, D. Cao, J. Gonzalez, S. Hadida, A. Hazlewood, J. Joubran, T. Knapp, L.R. Makings, M. Miller, T. Neuberger, E. Olson, V. Panchenko, J. Rader, A. Singh, J.H. Stack, R. Tung, P.D. Grootenhuis, and P. Negulescu. 2006. Rescue of DeltaF508-CFTR trafficking and gating in human cystic fibrosis airway primary cultures by small molecules. *Am J Physiol Lung Cell Mol Physiol*. 290:L1117-1130.

Wainwright, C.E., J.S. Elborn, B.W. Ramsey, G. Marigowda, X. Huang, M. Cipolli, C. Colombo, J.C. Davies, K. De Boeck, P.A. Flume, M.W. Konstan, S.A. McColley, K. McCoy, E.F. McKone, A. Munck, F. Ratjen, S.M. Rowe, D. Waltz, M.P. Boyle, T.S. Group, and T.S. Group. 2015. Lumacaftor-Ivacaftor in Patients with Cystic Fibrosis Homozygous for Phe508del CFTR. *N Engl J Med*. 373:220-231.

Wang, Y., T.W. Loo, M.C. Bartlett, and D.M. Clarke. 2007. Correctors promote maturation of cystic fibrosis transmembrane conductance regulator (CFTR)-processing mutants by binding to the protein. *J Biol Chem*. 282:33247-33251.

Ward, C.L., S. Omura, and R.R. Kopito. 1995. Degradation of CFTR by the ubiquitin-proteasome pathway. *Cell*. 83:121-127.

Witko-Sarsat, V., C. Delacourt, D. Rabier, J. Bardet, A.T. Nguyen, and B. Descamps-Latscha. 1995. Neutrophil-derived long-lived oxidants in cystic fibrosis sputum. *Am J Respir Crit Care Med*. 152:1910-1916.

Yan, Z., Z.A. Stewart, P.L. Sinn, J.C. Olsen, J. Hu, P.B. McCray, Jr., and J.F. Engelhardt. 2015. Ferret and pig models of cystic fibrosis: prospects and promise for gene therapy. *Hum Gene Ther Clin Dev*. 26:38-49.

Zhang, D., F. Ciciriello, S.M. Anjos, A. Carissimo, J. Liao, G.W. Carlile, H. Balghi, R. Robert, A. Luini, J.W. Hanrahan, and D.Y. Thomas. 2012. Ouabain Mimics Low Temperature Rescue of F508del-CFTR in Cystic Fibrosis Epithelial Cells. *Front Pharmacol*. 3:176.

Zhang, F., N. Kartner, and G.L. Lukacs. 1998. Limited proteolysis as a probe for arrested conformational maturation of delta F508 CFTR. *Nat Struct Biol*. 5:180-183.

Zhang, H., W. Wu, Y. Du, S.J. Santos, S.E. Conrad, J.T. Watson, N. Grammatikakis, and K.A. Gallo. 2004. Hsp90/p50cdc37 is required for mixed-lineage kinase (MLK) 3 signaling. *J Biol Chem*. 279:19457-19463.

Zhang, Z.R., J.S. Bonifacino, and R.S. Hegde. 2013. Deubiquitinases sharpen substrate discrimination during membrane protein degradation from the ER. *Cell*. 154:609-622.

Table 1: The list of corrector drugs used in this study with their corresponding known primary MOAs (related to Figure 1).

Drugs of the CFBE dataset (Reference for correction activity)	Primary Use/ Class
4-AN, PARP1 inhibitor (Anjos et al., 2012)	PARP1 inhibitor
ABT888 (Anjos et al., 2012)	A poly(ADP-ribose) polymerase (PARP) -1 and -2 inhibitor with chemosensitizing and antitumor activities. ABT-888 inhibits PARPs, thereby inhibiting DNA repair and potentiating the cytotoxicity of DNA-damaging agents.
Glafenine (Robert et al., 2010)	An anthranilic acid derivative with analgesic properties used for the relief of all types of pain (1)
GSK339 (D Y Thomas lab unpublished)	Androgen receptor ligand (Norris et al., 2009).
Ibuprofen (Carlile et al., 2015)	Ibuprofen is a nonsteroidal anti-inflammatory drug. It is a non-selective inhibitor of cyclooxygenase.
JFD03094	PARP inhibitor
KM11060 (Robert et al., 2008)	PDE5 inhibitor (an analog of sildenafil).
Latonduine (Carlile et al., 2012)	PARP3 inhibitor
Minocycline H (D Y Thomas lab unpublished)	A tetracycline analog that inhibits protein synthesis in bacteria. Also known to inhibit 5-lipooxygenase in the brain (2).
Ouabagenin (Zhang et al., 2012)	A cardiaoactive glycoside obtained from the seeds of *Strophanthus gratus*. Acts by inhibiting Na+/K+_ATPase, resulting in an increase in intracellular sodium and calcium concentrations (2).
Ouabain (Zhang et al., 2012)	A cardiaoactive glycoside obtained from the seeds of *Strophanthus gratus*. Acts by inhibiting Na+/K+ ATPase, resulting in an increase in intracellular sodium and calcium concentrations (2).
PJ34 (Anjos et al., 2012)	PARP1 inhibitor
Low temperature (Denning et al., 1992)	

Drugs of the MANTRA dataset (Reference for correction activity)	Primary Use/ Class
Chloramphenicol (Carlile et al., 2007)	Inhibitor bacterial protein synthesis by binding to 23S rRNA and preventing peptidyl transferase activity (2).
Chlorzoxazone (Carlile et al., 2007)	Muscle relaxant. Acts by inhibiting degranulation of mast cells and preventing the release of histamine and slow-reacting substance of anaphylaxis. It acts at the level of the spinal cord and subcortical areas of the brain where it inhibits multi-synaptic reflex arcs involved in producing and maintaining skeletal muscle spasm (2).
Dexamethasone (Caohuy et al., 2009)	Is a synthetic glucocorticoid agonist. Its anti-inflammatory properties are thought to involve phospholipase A_2 inhibitory proteins, lipocortins (2).
Doxorubicin (Maitra et al., 2001)	DNA intercalator that inhibits topoisomerase II activity by stabilizing the DNA-topoisomerase II complex (2).
Glafenine (Robert et al., 2010)	An anthranilic acid derivative with analgesic properties used for the relief of all types of pain (1).
Liothyronine (Carlile et al., 2007)	L-triiodothyronine (T3, liothyronine) thyroid hormone is normally synthesized and secreted by the thyroid gland. Most T3 is derived from peripheral monodeiodination of T4 (L-tetraiodothyronine, levothyroxine, L-thyroxine). The hormone finally delivered and used by the tissues is mainly T3. Liothyronine acts on the body to increase the basal metabolic rate, affect protein synthesis and increase the body's sensitivity to catecholamines (such as adrenaline). It is used to treat hypothyroidism (2).
MS-275 (Hutt et al., 2010)	Also known as Entinostat. An inhibitor of Class Ihistone deacetylases (preferentially HDAC 1, also HDAC 3) (Hu et al., 2003).
Scriptaid (Hutt et al., 2010)	An inhibitor of Class I histone deacetylases (HDAC1, HDAC3 and HDAC8) (Hu et al., 2003).
Strophanthidin (Carlile et al., 2007)	A cardioactive glycoside that inhibits Na+/K+_ATPase. Also known to inhibit the interaction of MDM2 and MDMX (1).
Thapsigargin (Egan et al., 2002)	A sesquiterpene lactone found in roots of *Thapsia garganica*. A non-competitive inhibitor of sarco/endoplasmic Ca^{2+} ATPase (SERCA) (1).
Trichostatin-A (Hutt et al., 2010)	An inhibitor of histone deacetylases (HDAC1, HDAC3, HDAC8 and HDAC7) (Hu et al., 2003).

1284

1285 (1) http://pubchem.ncbi.nlm.nih.gov/

1286 (2) www.drugbank.ca

1287

1288

Reference:

Anjos, S.M., Robert, R., Waller, D., Zhang, D.L., Balghi, H., Sampson, H.M., Ciciriello, F., Lesimple, P., Carlile, G.W., Goepp, J.*, et al.* (2012). Decreasing Poly(ADP-Ribose) Polymerase Activity Restores DeltaF508 CFTR Trafficking. Front Pharmacol *3*, 165.

Caohuy, H., Jozwik, C., and Pollard, H.B. (2009). Rescue of DeltaF508-CFTR by the SGK1/Nedd4-2 signaling pathway. J Biol Chem *284*, 25241-25253.

Carlile, G.W., Keyzers, R.A., Teske, K.A., Robert, R., Williams, D.E., Linington, R.G., Gray, C.A., Centko, R.M., Yan, L., Anjos, S.M.*, et al.* (2012). Correction of F508del-CFTR trafficking by the sponge alkaloid latonduine is modulated by interaction with PARP. Chem Biol *19*, 1288-1299.

Carlile, G.W., Robert, R., Goepp, J., Matthes, E., Liao, J., Kus, B., Macknight, S.D., Rotin, D., Hanrahan, J.W., and Thomas, D.Y. (2015). Ibuprofen rescues mutant cystic fibrosis transmembrane conductance regulator trafficking. J Cyst Fibros *14*, 16-25.

Carlile, G.W., Robert, R., Zhang, D., Teske, K.A., Luo, Y., Hanrahan, J.W., and Thomas, D.Y. (2007). Correctors of protein trafficking defects identified by a novel high-throughput screening assay. Chembiochem *8*, 1012-1020.

Denning, G.M., Anderson, M.P., Amara, J.F., Marshall, J., Smith, A.E., and Welsh, M.J. (1992). Processing of mutant cystic fibrosis transmembrane conductance regulator is temperature-sensitive. Nature *358*, 761-764.

Egan, M.E., Glockner-Pagel, J., Ambrose, C., Cahill, P.A., Pappoe, L., Balamuth, N., Cho, E., Canny, S., Wagner, C.A., Geibel, J.*, et al.* (2002). Calcium-pump inhibitors induce functional surface expression of Delta F508-CFTR protein in cystic fibrosis epithelial cells. Nature medicine *8*, 485-492.

Hu, E., Dul, E., Sung, C.M., Chen, Z., Kirkpatrick, R., Zhang, G.F., Johanson, K., Liu, R., Lago, A., Hofmann, G.*, et al.* (2003). Identification of novel isoform-selective inhibitors within class I histone deacetylases. J Pharmacol Exp Ther *307*, 720-728.

Hutt, D.M., Herman, D., Rodrigues, A.P., Noel, S., Pilewski, J.M., Matteson, J., Hoch, B., Kellner, W., Kelly, J.W., Schmidt, A.*, et al.* (2010). Reduced histone deacetylase 7 activity restores function to misfolded CFTR in cystic fibrosis. Nat Chem Biol *6*, 25-33.

Maitra, R., Shaw, C.M., Stanton, B.A., and Hamilton, J.W. (2001). Increased functional cell surface expression of CFTR and DeltaF508-CFTR by the anthracycline doxorubicin. Am J Physiol Cell Physiol *280*, C1031-1037.

Norris, J.D., Joseph, J.D., Sherk, A.B., Juzumiene, D., Turnbull, P.S., Rafferty, S.W., Cui, H., Anderson, E., Fan, D., Dye, D.A.*, et al.* (2009). Differential presentation of protein interaction surfaces on the androgen receptor defines the pharmacological actions of bound ligands. Chem Biol *16*, 452-460.

Robert, R., Carlile, G.W., Liao, J., Balghi, H., Lesimple, P., Liu, N., Kus, B., Rotin, D., Wilke, M., de Jonge, H.R.*, et al.* (2010). Correction of the Delta phe508 cystic fibrosis transmembrane conductance regulator trafficking defect by the bioavailable compound glafenine. Mol Pharmacol *77*, 922-930.

Robert, R., Carlile, G.W., Pavel, C., Liu, N., Anjos, S.M., Liao, J., Luo, Y., Zhang, D., Thomas, D.Y., and Hanrahan, J.W. (2008). Structural analog of sildenafil identified as a novel corrector of the F508del-CFTR trafficking defect. Mol Pharmacol *73*, 478-489.

Zhang, D., Ciciriello, F., Anjos, S.M., Carissimo, A., Liao, J., Carlile, G.W., Balghi, H., Robert, R., Luini, A., Hanrahan, J.W.*, et al.* (2012). Ouabain Mimics Low Temperature Rescue of F508del-CFTR in Cystic Fibrosis Epithelial Cells. Front Pharmacol *3*, 176.

Table 2: MLK3 pathway regulates the proteostasis of mutant proteins that are structurally related to CFTR.

Mutant Proteins	Correction (% of wild type) *	
	Control (DMSO)	JNKi II (5μM)
P-Glycoprotein DY490	24	44
hERG R948X	44	24
NCC G601S	10	9
ATP7B H1069Q	32	80
ATP7B R778L	12	40
Note: * in case of ATP7B mutants denotes fraction of protein in Golgi as calculated by fluorescence microscopy, and in other cases the protein that was processed by the Golgi are calculated by a biochemical assay similar to the one used for CFTR.		

CFBE or HeLa cells (in case of ATP7B) were transfected with constructs encoding the indicated mutant proteins and treated with JNKi II for 48h. The effect of JNKiII on proteostasis of these mutants was monitored by western blotting (to measure the change in Golgi processed band C or ER localized band B; see Figure S5F) or in the case of ATP7B using fluorescence microscopy to monitor the efficiency of translocation of the ER-localized mutant proteins to the Golgi. Treatment with JNKi II corrects the folding-trafficking defects of mutant proteins that have similar structure to F508del-CFTR (P-gp and ATP7B) while it does not have any effect or has an opposite effect on other multi-transmembrane proteins. ATP7B mutants displayed efficient correction after downregulation of the MLK3 pathway, where the localization of the mutant proteins to the Golgi reached almost the WT levels. The data on ATP7B are published elsewhere (Chesi et al submitted).

Figure legends:

Figure 1: Corrector drugs modulate a set of CORE genes.

A. Schema of the FIT method. The upregulated (red) and downregulated genes (blue) were fuzzy intersected to identify CORE genes.

B. The number of probe sets in the corrector drug profiles (MANTRA dataset) as well as random profiles from MANTRA database were intersected with variable fuzzy cut-offs (represented as number of drugs out of 11) to obtain optimal fuzzy cut-off for the analysis. The enlargement (inset) shows that at the optimal fuzzy cut-off (0.7; 8 out of 11 drugs), the signal-to-noise ratio was close to 3 (108 probe-sets in the corrector drug intersection vs 32 in the random drug intersection).

C. At a fuzzy cut-off of 0.7, the number of random drug profiles used was varied, and the number of probe-sets present in the intersection is shown.

D. Using the optimal parameters (see B, C) the FIT analysis resulted in 402 upregulated and 219 downregulated CORE genes.

E. The number of CORE genes associated with the enriched GO terms is shown. Those genes that did not associate with enriched GO terms were excluded from the chart.

F. Protein-protein interactions between the CORE and the proteostasis genes (restricted to those that connect the two groups) are shown.

Figure 2: Validation of the selected CORE genes.

A-D. CFBE cells were treated with siRNAs targeting CORE genes and changes in F508del-CFTR proteostasis monitored by western blotting. The fold change in the levels of band C obtained by downregulating anti-correction (A) and pro-correction (D) genes and the fold change in levels of band B (B) and band C/ band B ratio (C) after

downregulation of the anti-correction genes are shown. The effects of negative control siRNAs (dashed line) and VX-809 (green) are indicated.

E. The validated CORE genes (blue – pro-correction hits, orange – anti-correction hits, and grey – no action) were assembled into coherent networks based on information from databases. Non-directional interactions denote protein-protein interaction, directional interactions represent phosphorylation cascades and dashed arrows indicate indirect connections through intermediaries.

F. Western blot of CFBE cells treated with mitoxantrone (2.5 to 20 μM for 48h), a potential corrector identified using downregulation of anti-corrector genes as selection criteria. Mitoxantrone increased the levels of both band C and band B.

G. Treatment of CFBE cells with the indicated combinations of siRNAs targeting CORE genes led to a synergistic increase in the band C levels. Changes in the levels of band C were quantitated from western blotting are presented as mean ±SEM (n > 3). The representative blots are shown in the insert, the upper panel corresponds to a blot with lower exposure where the differences in band C levels can be easily appreciated, while the bottom panel corresponds to a blot with higher exposure where a faint band C can be seen even under control siRNA treatment.

Figure 3: Delineation of the MLK3 pathway branch that controls F508del-CFTR proteostasis.

A. CFBE cells were treated with indicated siRNAs targeting the upstream activators of MLK3 and their effect on F508del-CFTR proteostasis monitored by western blotting. The fold change in band C levels are shown as mean ±SEM (n > 3). Reduction in TGF receptor, HPK, CDC42 and RAC2 levels rescued F508del-CFTR from ERQC. The

rescue obtained with TNFR2 siRNA was quite variable and so it was not considered further.

B. JNK isoforms were tested for their effect on F508del-CFTR proteostasis after siRNA-mediated downregulation of their levels. Downregulation of JNK2 leads to efficient rescue of F508del-CFTR that is comparable to that obtained with MLK3. The fold change in band C levels are presented as mean ±SEM (n > 3) with western blot in the insert.

C. CFBE cells were transfected with activators of the MLK3 pathway to study their effect on F508del-CFTR proteostasis. The fold change in the band B levels are shown as mean ±SEM (n > 3) with western blot in the insert. All of them reduced the levels of both band B and band C (not shown) of F508del-CFTR. The corresponding increase in the levels of phospho-c-jun indicates an increase activation of the MLK3 pathway activity.

D-E. Schematic representation of the proposed MLK3 (D) and CAMKK2 (E) pathways that regulate F508del-CFTR proteostasis. The directional interactions proposed between the components of the pathways are based on published literature.

Figure 4: MLK3 pathway regulates the degradation of F508del-CFTR.

A-B. CFBE cells pretreated with siRNAs were treated with CHX (50 μg/mL) for indicated times and the levels of band B of F508del-CFTR was monitored (A). The levels were quantitated and represented in (B) as mean ±SEM (n > 3). Downregulation of MLK3 or JNK2 reduced the kinetics of reduction of band B of F508del-CFTR.

C-D. CHX chase assay (see above) after overexpression of the activators of MLK3 pathway. The activation of MLK3 pathway increases the rate of degradation of band B (C). Quantitation of the blot is shown in (D) as mean ±SEM (n > 3).

E-F. CFBE cells were treated with indicated siRNAs followed by incubation at 26 °C for 6h followed by shift to 37 °C for the indicated time periods. The changes in band C levels

were monitored as measure of PQC (C). See (F) for quantitation of band C levels represented as mean ±SEM (n > 3).

G-H. PQC assay (see above) after overexpression of CDC42 or JNK2 shows an increased rate of degradation of band C (G) upon CDC42 overexpression. JNK2 overexpression has no effect on the PQC of F508del-CFTR. The blots were quantified and presented in (H) as mean ±SEM (n > 3).

Figure 5: ROS and inflammatory cytokines control F508del-CFTR proteostasis via the MLK3 pathway.

A. CFBE cells (pre-treated with MLK3 siRNA) were treated with 1 mM H_2O_2 for 30 min and levels of band B monitored by western blotting. Control cells show drastic reduction in F508del-CFTR levels upon treatment with H_2O_2 that is prevented by the downregulation of MLK3.

B. Quantitation of band B levels from (A) represented as mean ±SEM (n > 3).

C. CFBE cells (pre-treated with MLK3 siRNA) were treated with 50 ng/mL of TNF-α or TGF-β for 15min and levels of band B monitored by western blotting. MLK3 downregulation prevents the decrease in band B levels brought about by treatment with the cytokines.

D. Quantitation of the band B levels from (C) represented as mean ±SEM (n > 3).

Figure 6: Inhibitors of the MLK3 pathway rescue F508del-CFTR.

A-D. CFBE cells were treated with the indicated inhibitors of the MLK3 pathway or VX-809 for 48 h, and the rescue of F508del-CFTR from ERQC was monitored (A). MLK3 pathway inhibitors rescue F508del-CFTR to levels comparable to or more than that achieved by VX-809. Changes in the levels of band C (B), band B (C) and the band C/band B ratio (D) were quantitated and shown mean ±SEM (n > 3). Normalized

concentration (abscissa in panels B-D) refers to concentration [VX-809, JNKi IX and Oxozeaenol (1.25, 2.5, 5, 10 μM), JNKi II (6.25,12.5, 25, 50 μM), JNKi XI (3.12, 6.25,12.5, 25 μM)] values that were normalized to the maximum used concentrations of the respective drugs. Refer panel A for concentrations (μM) of the drugs used.

E. CFBE cells were treated with inhibitors of the MLK3 pathway and/or VX-809 (5μM) for 48 h and changes in band C levels monitored. The concentrations of the MLK3 pathway inhibitors used were: JNKi II (12.5μM), JNKi IX (5μM), JNKi XI (25μM) and oxozeaenol (5μM). Wild type CFTR (wt-CFTR) was used as a control.

F. Quantitation of band C levels from (E) normalized to the levels of band C after VX-809 treatment are shown as mean ±SEM (n > 3). The results show that synergy obtained between the MLK3 pathway inhibitors and VX-809 brings the levels of band C to about 40% of the wild type levels.

Figure 1- figure supplement 1: Corrector drugs (MANTRA dataset) have diverse transcriptional responses corresponding to their primary MOA.

As noted earlier, the correctors had few if any common principal MOA. First, we wished to identify sub-groups of correctors, if any, which might have shared correction-relevant MOA. The use of prototype ranked lists (PRLs) for the correctors present in the MANTRA dataset (Iorio et al., 2010) results in the loss of information about fold-changes in transcript levels and corresponding p-values. Thus, these lists are not suitable for comparisons and cluster analyses made with traditional metrics (such as Correlation or Euclidian distance) and classic partitional or agglomerative/hierarchical clustering methods. However, we attempted to overcome this issue by a state-of-the-art method to "cluster" the profiles. In the past, in an effort to cluster the drugs present in the

connectivity map database (Iorio et al., 2010) based on their transcriptional response similarity, we had designed a novel Gene set enrichment analysis (GSEA: (Subramanian et al., 2005)) based metric to obtain similarity scores between ranked lists [see (Iorio et al., 2010) for details]. This study resulted in a network that contains clusters of densely interconnected drugs (named drug communities), whose corresponding ranked-lists had high “similarity” scores. Since this network is basically the output of a state-of-the-art method to cluster the ranked-lists of genes derived from connectivity map, we mined this network in an attempt to cluster the F508del-CFTR corrector drugs. Shown here is the drug similarity network assembled, by iterative affinity propagation clustering. The topology of this network is hierarchical and derived from a gene set enrichment analysis (GSEA)-derived similarity metric applied to drug-induced transcriptional profiles (see (Iorio et al., 2010) for details). Each node represents a drug. An edge connects two nodes if the corresponding consensual transcriptional responses are significantly similar and its length is inversely proportional to the similarity of the response. The clusters (referred to as drug-communities) correspond to drugs with highly similar transcriptional responses. The F508del-CFTR correctors belonging to this network (from MANTRA dataset) are highlighted together with the identifier of the drug-community they belong to. The nodes (corrector drugs) are color-coded such that drugs belonging to the same community share the same color. The F508del-CFTR correctors do not cluster together and most of them belong to drug-communities enriched for their primary MOA (Supplementary File 2).

Figure 1- figure supplement 2: IPA based analysis uncovers networks of CORE genes.

The CORE genes were analyzed by the IPA-Core analysis function both together and individually as up and downregulated gene sets. Among the networks built by IPA using

1510 the downregulated CORE genes set, 4 significant ones are shown. The downregulated
1511 CORE genes are shown in grey while the nodes that were predicted by IPA to be part of
1512 the network are shown in white. The nodes predicted by IPA include NF-KB, AKT, VEGF
1513 and PI3K complexes. The differences in the shape of the nodes indicate the protein
1514 families to which the nodes belong (see the panel legend for details). The blue circles
1515 indicate the network hubs that were tested in the screening assay (see Figure 2A-D).
1516
1517 **Figure 2- figure supplement 1: Characterization of biochemical assay to monitor**
1518 **F508del-CFTR correction.**
1519 A. The changes in the F508del-CFTR proteostasis were monitored by a biochemical
1520 assay. This assay is sensitive and robust enough to detect even small changes in the
1521 proteostasis of CFTR.
1522 CFTR is resolved by SDS-PAGE into two distinct bands - one at ~ 140 kDa (band B;
1523 core glycosylated protein present in the ER) and another at ~ 170 kDa (band C;
1524 processed by Golgi-localized glycosylation enzymes). In the case of wild type CFTR, the
1525 majority of the protein is in the form of band C (not shown) while in the case of mutant
1526 F508del-CFTR the major form is band B. Sometimes a lower molecular weight band,
1527 termed band A is also observed that probably corresponds to non-glycosylated CFTR.
1528 For the quantitation's described in this manuscript, bands B and A were considered
1529 together as band B. Quantitation of the changes in the levels of bands B and C were
1530 carried out as outlined here in this example. CFBE cells were treated with indicated
1531 corrector drugs for 48h and were lysed and processed for western blotting as described
1532 materials and methods. Treatment with corrector drugs increases the levels of both band
1533 B and band C of F508del-CFTR. Na+/K+ ATPase was used as loading control. To
1534 quantitate the levels of bands B and C, the x-ray films obtained were scanned using a

flatbed scanner (Hewlett-Packard) at a resolution of 200-600 dpi and exported as 8-bit .tiff images.

B. The scanned images were then imported into ImageJ for quantitation. First, the images were converted to grey scale and background of the image was removed using the “subtract background” function with a rolling ball radius of 50-150 pixels. Next, using the rectangular selection tool, C band’s (shown here) or B band’s were selected.

C. The gel/blot analysis tool (Analyze>Gels) was then used for quantitation of the selected bands. First the “select first lane” function was executed followed by the “plot lane” function. This resulted in a plot as shown here. The area under the curve (as a measure of the density of bands) was then quantitated using the magic wand tool to select the peaks individually and exporting the density into a text file. The quantitated density values are indicated below the plot. We note that the method described here is semi-quantitative; nevertheless, the values obtained adequately describe the biological phenomenon observed.

D. The fold change in band C levels calculated using the measured values of density in (C) are plotted. E, F. To test if the semi-quantitative process described here is within the linear range of detection, we resolved indicated quantities of cell lysates prepared from CFBE cells by SDS-PAGE followed by western blotting and the blots were processed as described before. The exposure time of the blots to the x-ray films was varied to get different intensity levels of the bands. Only one exposure of 30 sec is shown here (E) for clarity. The intensity of the bands was calculated using ImageJ (see above) and expressed as fold change in band B (E) relative to the minimum value. As can be noted, the amounts of band B quantitated are linear in the range from 10 to 80µg of cell lysate loaded. Similar results were obtained for band C. The linearity was also preserved for exposures that were twice or half of the time shown here. For experiments described in

this manuscript the total amount of protein loaded ranged from 25-40µg and exposure time of blots ranged from 30-45 sec.

Figure 2- figure supplement 2: Downregulation of CORE genes rescues F508del-CFTR more efficiently than the corrector drugs used originally, without altering the F508del-CFTR mRNA levels.

A. CFBE cells were treated with indicated corrector drugs for 48h and then lysed and prepared for western blotting, to assay the rescue of F508del-CFTR from ERQC. The changes in the levels of band C after drug treatment are shown as mean ±SEM (n > 3).

B. CFBE cells were treated with indicated siRNAs (targeting the anti-correction genes) for 72h, and then total RNA from the cells was purified. The levels of CFTR mRNA were quantitated by RT-PCR. The data is presented as mRNA levels relative to the negative control siRNAs. The values are expressed as mean ±SEM (n = 4).

C. Representative blot used for quantitations represented in Figure 2A-C.

D. Representative blot used for quantitations represented in Figure 2D

Figure 2- figure supplement 3: The siRNAs efficiently reduce the transcript levels of their target genes.

A. CFBE cells were treated with indicated siRNAs for 72 h. The efficiency of silencing for each gene was evaluated by quantitative RT-PCR and expressed as fold-change represented as mean ±SEM (n = 3). The siRNA treatment reduced the mRNA levels of the target genes to about 10-30% of the levels present in control cells treated with non-targeting siRNA.

B. CFBE cells were treated with the indicated doses of siRNAs targeting the CORE genes for 72h. The change in the mRNA levels of the CORE genes was quantitated by RT-PCR and expressed as fold change represented as mean ±SEM (n > 3). The effect

on F508del-CFTR proteostasis was also monitored by western blotting and shown in the insert. There was a positive correlation between the reduction in the levels of CORE genes and the change in proteostasis of F508del-CFTR.

Figure 3- figure supplement 1: Delineation of the MLK3 and CAMKK2 pathway branches that regulate F508del-CFTR proteostasis.

A. HeLa cells [HeLa cells stably expressing HA-tagged F508del-CFTR] were treated with indicated siRNAs targeting MLK3 pathway components including p38 MAPK (mix of siRNAs targeting all 4 isoforms) and JNK (mix of siRNAs targeting all 3 JNKs). The effect on F508del-CFTR proteostasis monitored by western blotting. Fold Change in the levels of band C was quantitated and presented as mean ±SEM (n > 3) with a representative blot shown in the insert. The downregulation of the MLK3 pathway components (including p38 MAPK) leads to the rescue of F508del-CFTR in HeLa cells. SiRNAs targeting Rma1 and Aha1 used as positive controls for rescue of F508del-CFTR.

B. Screening for F508del-CFTR proteostasis regulators among the CORE genes led to the identification of CAMKK2 as an anti-correction hit. Three downstream components and 9 upstream components of the CAMKK2 signaling pathway (as derived from literature mining) were tested, by siRNA-mediated downregulation, for their role in regulation of F508del-CFTR proteostasis. CFBE cells were treated with the indicated siRNAs for 72h and their effect on F508del-CFTR proteostasis monitored by western blotting. Four of them (CALML5, ITPR2, CAMK4 and AMPK [by a mix of siRNAs targeting PRKAA1 and PRKAA2]) rescued F508del-CFTR from ERQC as seen by an increase in band C levels.

C. The changes in the levels of band C from (B) were quantitated and are represented as mean ±SEM (n > 3). See Figure 3 for a representation of the derived CAMKK2 pathway that regulates F508del-CFTR proteostasis.

Figure 4- figure supplement 1: Characterization of the mode of action of the MLK3 pathway on F508del-CFTR proteostasis.

A-B. CFBE cells treated with MLK3 siRNA were pulsed with radioactive [35S]-cysteine and methionine for 15 min, and then chased for the indicated times. CFTR was immunoprecipitated and processed for autoradiography (A). The signals corresponding to band B from (A) were quantitated and presented in (B). The data are representative of 2 independent experiments. Note the reduced degradation of F508del-CFTR upon downregulation of MLK3.

C. Down-regulation of the MLK3-JNK pathway does not affect the activity of proteasomes. CFBE cells treated with MLK3 or JNK2 siRNA for 72h were transfected with Proteasome ZsProsensor-1 for the final 24 h, and the levels Proteasome ZsProsensor-1 monitored by fluorescence microscopy. Treatment with MG132 (20 µg/ml for 3h), a proteasomal inhibitor, was used as a positive control. While treatment with MG132 increases the fluorescence levels of ZsProsensor-1 compared to untreated cells indicating a reduced proteasome activity, downregulation of MLK3 or JNK2 did not change the levels of fluorescence, suggesting that proteasome activity is not changed under these conditions.

D. CFBE cells were treated with MLK3 or JNK2 siRNA and processed for western blotting to monitor the accumulation of poly ubiquitinated proteins. There was no change in the levels of poly ubiquitinated proteins suggesting that these treatments do not affect proteasome activity.

E. Down-regulation of MLK3 does not affect the folding of F508del-CFTR. CFBE cells expressing wild type CFTR or F508del-CFTR were treated with MLK3 siRNA as indicated. Untreated CFBE cells incubated at 26 °C for 24h were used as a positive control for the promotion of folding. Membrane fractions from the cells were isolated and subjected to trypsin digestion for 10 min on ice, followed by western blotting with M3A7

antibody that recognizes the NBD2 domain of F508del-CFTR, or with 3G11 antibody that recognizes NBD1. The wild-type CFTR and its NBD domains show more resistance to trypsin digestion compared to F508del-CFTR. There was no change in the stability of F508del-CFTR or its NBD domains upon down-regulation of MLK3, while the low temperature treatment enhanced the stability of F508del-CFTR and its NBD1 domain. The western blots are representative of at least 3 different experiments.

F. Down-regulation of MLK3 does not affect the exit of cargo from the ER. CFBE cells were treated with MLK3 siRNA for 72 h, and during the final 16 h they were transfected with VSVG-GFP and incubated at 40 °C. The cells were then shifted to 32 °C to allow the exit of cargoes from the ER. The cells were fixed at the indicated times after shift to 32 °C and labeled for GM130 (red) to mark the Golgi apparatus and DAPI (blue) to stain the nucleus. The rate of transport of VSVG-GFP (green) either from ER to Golgi or from Golgi to the PM was not significantly affected by the downregulation of MLK3. Bar = 20 μm.

G. HeLa cells were treated with JNKi II (2.5μM) for 24h and F508del-CFTR was immunoprecipitated. The immunoprecipitate was subjected to western blotting to reveal the amount of associated HOP. The blots (like in the insert) were quantitated and normalized to the levels of F508del-CFTR (not shown). The values are presented as mean ±SD (n>3).

Figure 6- figure supplement 1: Small-molecule inhibitors of the MLK3 pathway rescue

F508del-CFTR and other structurally related mutant proteins from degradation.

A. CFBE cells were treated with indicated JNK inhibitors for 24h and processed for western blotting. The levels of phospho-c-jun as a measure of JNK inhibition was

monitored. MLK3 pathway inhibitors reduce phospho-c-jun levels efficiently indicating a strong reduction in the activity of JNK and hence presumably of the MLK3 pathway.

B. CFBE cells were treated with TAK1 or MLK3 siRNA as indicated and changes in F508del-CFTR proteostasis were monitored by western blotting. TAK1 does not regulate F508del-CFTR proteostasis, as evidenced by the absence of change in the levels of bands C or B. The fold change in the band C levels were quantitated and plotted as mean ±SD (n = 2).

C. CFBE cells were treated with 5 μM oxozeaenol for 48 h, or with MLK3 siRNA, or with both, and the correction of the F508del-CFTR folding/ trafficking defect was monitored by changes in the levels of band C. There was no additive effect observed with the combination of MLK3 downregulation and oxozeaenol treatment. The quantitated band C levels are expressed as mean ±SD (n > 3).

D. CFBE cells were treated with 5 μM oxozeaenol for 24 h, and the activity of the JNK pathway was measured by western blotting for phospho c-jun levels and F508del-CFTR. The levels of phospho c-jun were reduced suggesting that oxozeaenol leads to a reduction in the activity of JNK. The increase in band C levels of F508del-CFTR show that the reduction in the activity of JNK is accompanied by a rescue of F508del-CFTR from ERQC.

E. CFBE cells were treated with flunarizine (at concentrations 6.25-50μM) targeting the CAMKK2 pathway for 48h and the effect on F508del-CFTR proteostasis measured by western blotting. Treatment with flunarizine increased the levels of band C of F508del-CFTR. Other small molecules known to inhibit the CAMKK2 pathway components (verapamil and STO-609) did not show any effect on correction of F508del-CFTR.

F. CFBE cells transiently transfected with the P-glycoprotein mutant (P-gp DY490), the NCC mutant (R948X), or the hERG mutant (G601S) were treated with JNKi II for 24 h, and the effect of the drug on their proteostasis monitored by western blotting. While the

trafficking of P-gp DY490 out of the ER was enhanced by this treatment (seen as an increase in the Golgi-associated band C, indicated by arrows), other mutants are subjected to enhanced degradation upon drug treatment, as shown by a decrease in the levels of both bands B and C.

G. CFBE cells were treated with JNKi II at indicated concentrations (25, 50 μM) for 48 h and the changes in the proteostasis of non-mutant endogenous proteins like E-cadherin, IGF1Rß and EGFR were monitored by western blotting. There was no significant change in the proteostasis of these proteins.

Figure 6- figure supplement 2: Small molecule inhibitors of MLK3 pathway rescue channel function of F508del-CFTR.

A. CFBE-YFP cells were treated with MLK3 pathway inhibitors and/or VX-809 for 48 h, and the anion transport measured as described in the materials and methods. The rate constants of the decrease in YFP fluorescence (K), a measure of anion conductance, after inhibitor treatments are shown. The data are expressed as mean ±SEM (n > 3).

B. Anion transport was measured in CFBE-YFP cells after downregulating the MLK3 pathway activity by siRNA-mediated knockdown MLK3 or JNK2. The rate constants of the decrease in YFP fluorescence (K), a measure of anion conductance, after downregulation of the indicated MLK3 pathway components are shown. The data are expressed as mean ±SEM (n > 3). Treatment with VX-809 was used as a positive control for the rescue.

C. CFBE41o- cells were grown under polarizing conditions before addition of oxozeaenol at indicated concentrations for 48 h, followed by the measurement of short circuit currents using Ussing chamber assays (see materials and methods). The columns show the measured values of the short circuit current after oxozeaenol treatment at the indicated concentrations. The values are mean ±SEM (n>3).

1716

Figure 1

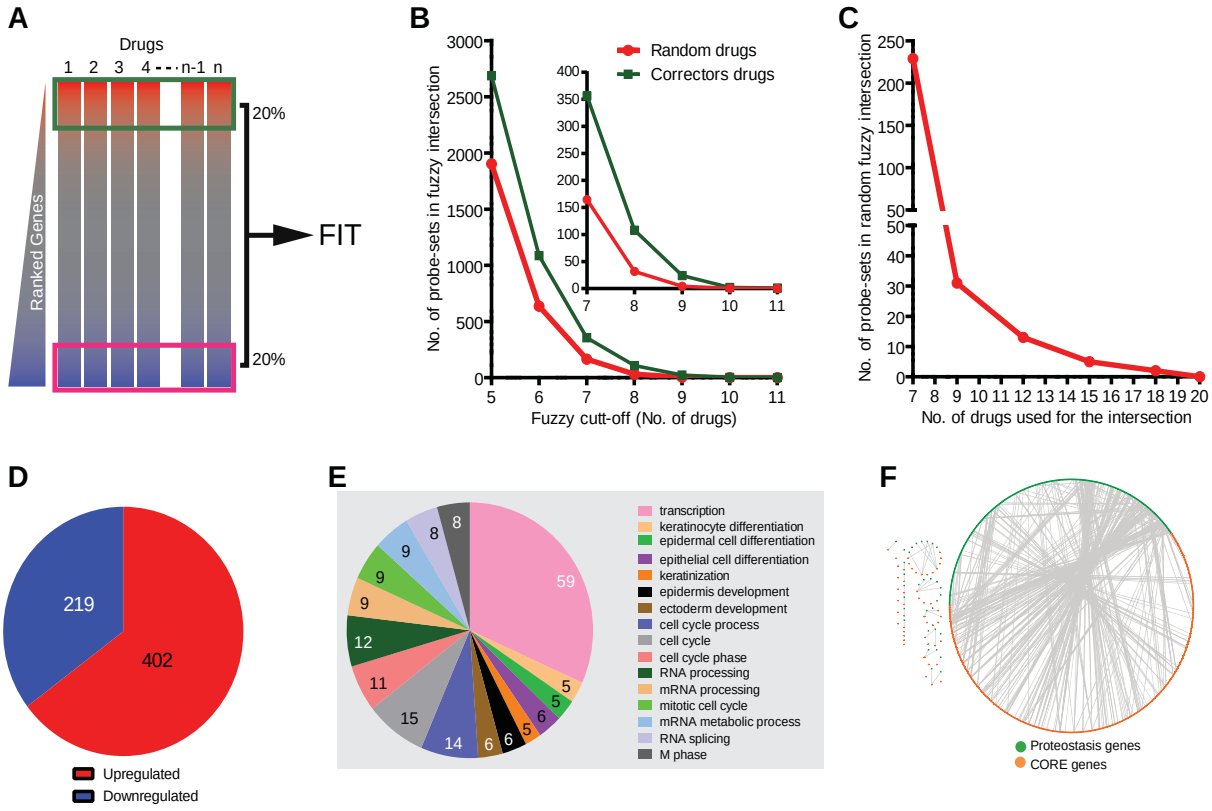
A
Drugs
1 2 3 4 n-1 n
Ranked Genes
20%
20%
FIT
B
Random drugs
Correctors drugs
No. of probe-sets in fuzzy intersection
Fuzzy cutt-off (No. of drugs)
C
No. of probe-sets in random fuzzy intersection
No. of drugs used for the intersection
D
219
402
Upregulated
Downregulated
E
59
5
5
6
5
6
6
14
15
11
12
9
9
8
8
transcription
keratinocyte differentiation
epidermal cell differentiation
epithelial cell differentiation
keratinization
epidermis development
ectoderm development
cell cycle process
cell cycle
cell cycle phase
RNA processing
mRNA processing
mitotic cell cycle
mRNA metabolic process
RNA splicing
M phase
F
Proteostasis genes
CORE genes

Figure 2

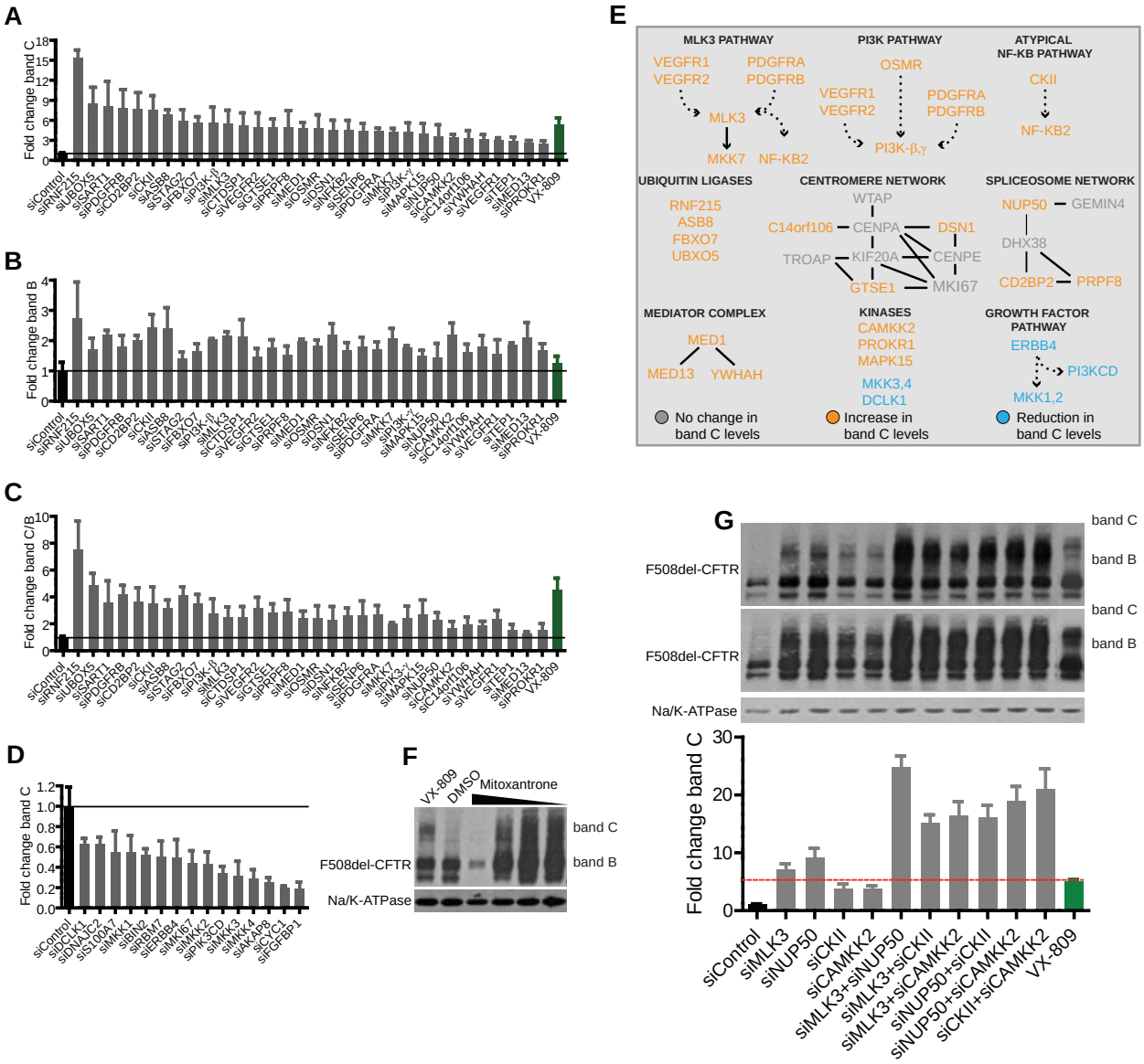
A
Fold change band C
B
Fold change band B
C
Fold change band C/B
D
Fold change band C
E
MLK3 PATHWAY
VEGFR1
VEGFR2
PDGFRA
PDGFRB
MLK3
MKK7
NF-KB2
PI3K PATHWAY
OSMR
VEGFR1
VEGFR2
PDGFRA
PDGFRB
PI3K-β,γ
ATYPICAL NF-KB PATHWAY
CKII
NF-KB2
UBIQUITIN LIGASES
RNF215
ASB8
FBXO7
UBXO5
CENTROMERE NETWORK
WTAP
C14orf106
CENPA
DSN1
TROAP
KIF20A
CENPE
GTSE1
MKI67
SPLICEOSOME NETWORK
NUP50
GEMIN4
DHX38
CD2BP2
PRPF8
MEDIATOR COMPLEX
MED1
MED13
YWHAH
KINASES
CAMKK2
PROKR1
MAPK15
MKK3,4
DCLK1
GROWTH FACTOR PATHWAY
ERBB4
PI3KCD
MKK1,2
No change in band C levels
Increase in band C levels
Reduction in band C levels
F
VX-809
DMSO
Mitoxantrone
band C
band B
F508del-CFTR
Na/K-ATPase
G
band C
band B
F508del-CFTR
band C
band B
F508del-CFTR
Na/K-ATPase
Fold change band C
siControl
siMLK3
siNUP50
siCKII
siCAMKK2
siMLK3+siNUP50
siMLK3+siCKII
siMLK3+siCAMKK2
siNUP50+siCKII
siNUP50+siCAMKK2
siCKII+siCAMKK2
VX-809

Figure 3

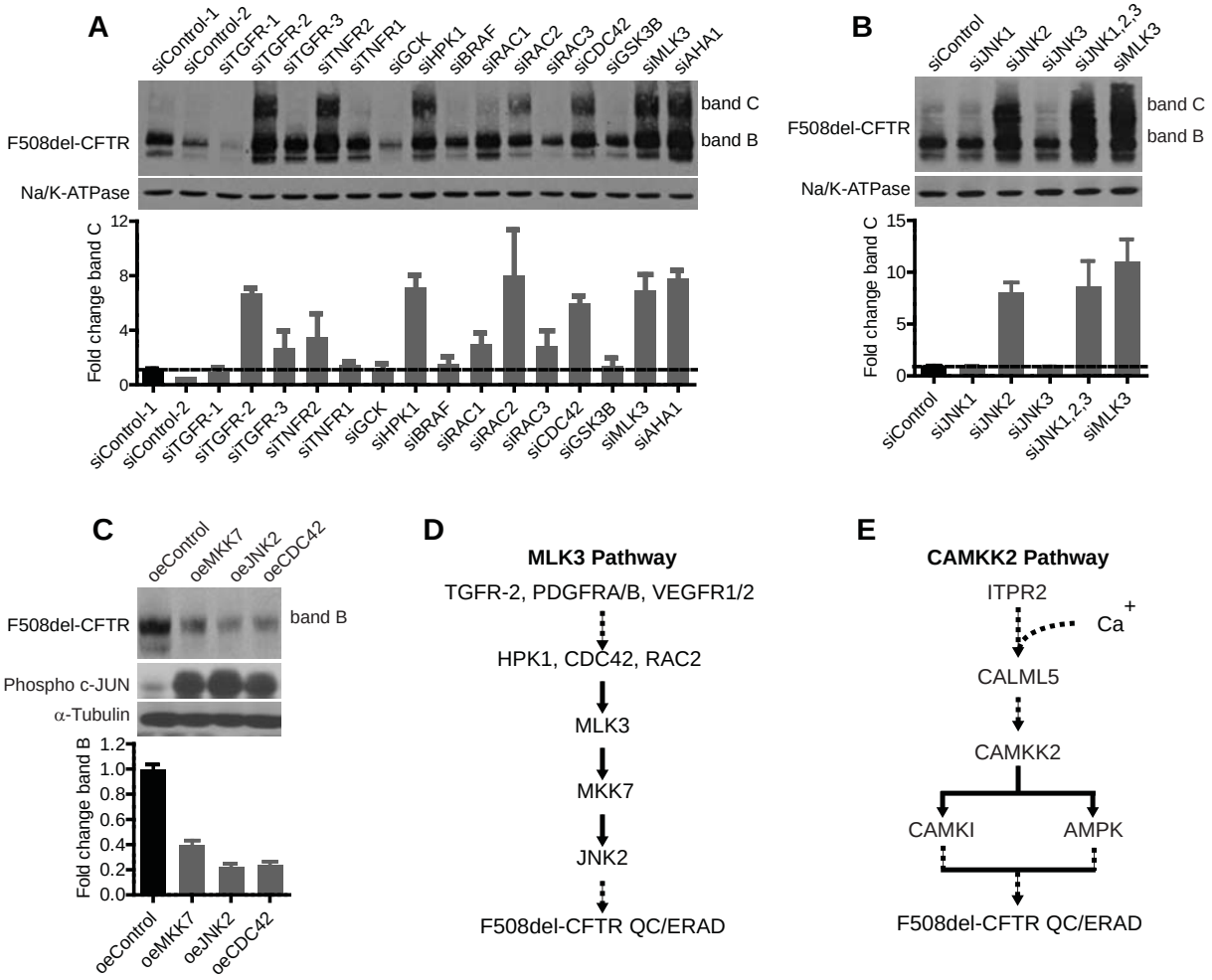
A
siControl-1
siControl-2
siTGFR-1
siTGFR-2
siTGFR-3
siTNFR2
siTNFR1
siGCK
siHPK1
siBRAF
siRAC1
siRAC2
siRAC3
siCDC42
siGSK3B
siMLK3
siAHA1
F508del-CFTR
band C
band B
Na/K-ATPase
Fold change band C
B
siControl
siJNK1
siJNK2
siJNK3
siJNK1,2,3
siMLK3
C
oeControl
oeMKK7
oeJNK2
oeCDC42
Phospho c-JUN
α-Tubulin
Fold change band B
D
MLK3 Pathway
TGFR-2, PDGFRA/B, VEGFR1/2
HPK1, CDC42, RAC2
MLK3
MKK7
JNK2
F508del-CFTR QC/ERAD
E
CAMKK2 Pathway
ITPR2
Ca+
CALML5
CAMKK2
CAMKI
AMPK
F508del-CFTR QC/ERAD

Figure 4

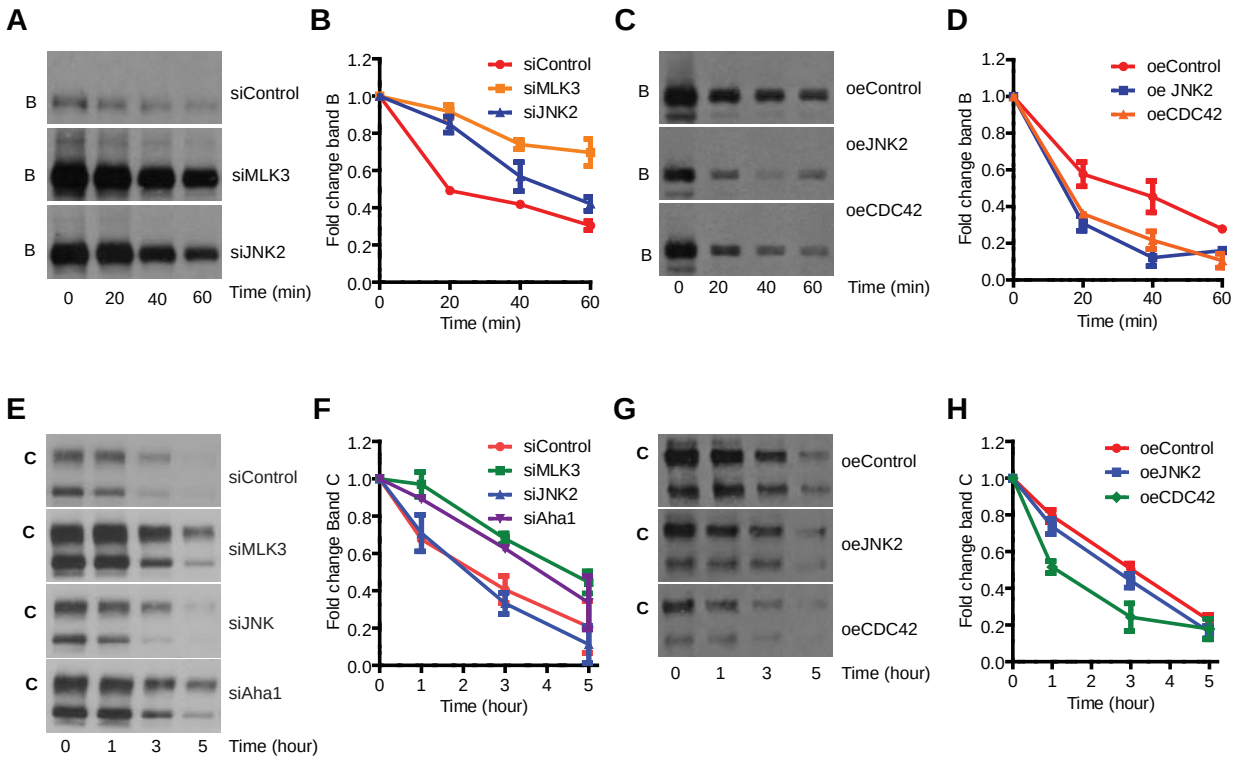
A
B
siControl
B
siMLK3
B
siJNK2
0 20 40 60
Time (min)
B
Fold change band B
siControl
siMLK3
siJNK2
Time (min)
C
B
oeControl
B
oeJNK2
B
oeCDC42
0 20 40 60
Time (min)
D
Fold change band B
oeControl
oe JNK2
oeCDC42
Time (min)
E
C
siControl
C
siMLK3
C
siJNK
C
siAha1
0 1 3 5
Time (hour)
F
Fold change Band C
siControl
siMLK3
siJNK2
siAha1
Time (hour)
G
C
oeControl
C
oeJNK2
C
oeCDC42
0 1 3 5
Time (hour)
H
Fold change band C
oeControl
oeJNK2
oeCDC42
Time (hour)

Figure 5

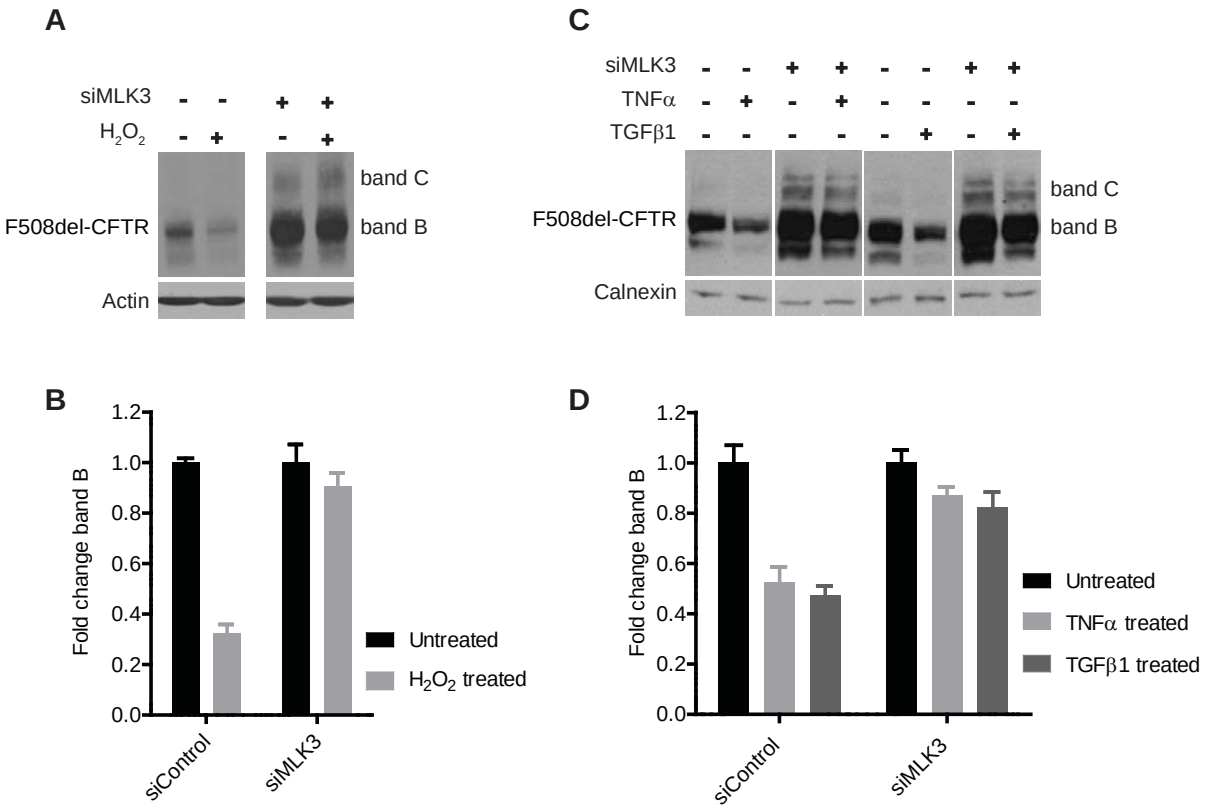
A
siMLK3 - - + +
H2O2 - + - +
band C
band B
F508del-CFTR
Actin
C
siMLK3 - - + + - - + +
TNFα - + - + - - - -
TGFβ1 - - - - - + - +
band C
band B
F508del-CFTR
Calnexin
B
Fold change band B
1.2
1.0
0.8
0.6
0.4
0.2
0.0
Untreated
H2O2 treated
siControl
siMLK3
D
Fold change band B
1.2
1.0
0.8
0.6
0.4
0.2
0.0
Untreated
TNFα treated
TGFβ1 treated
siControl
siMLK3

Figure 6

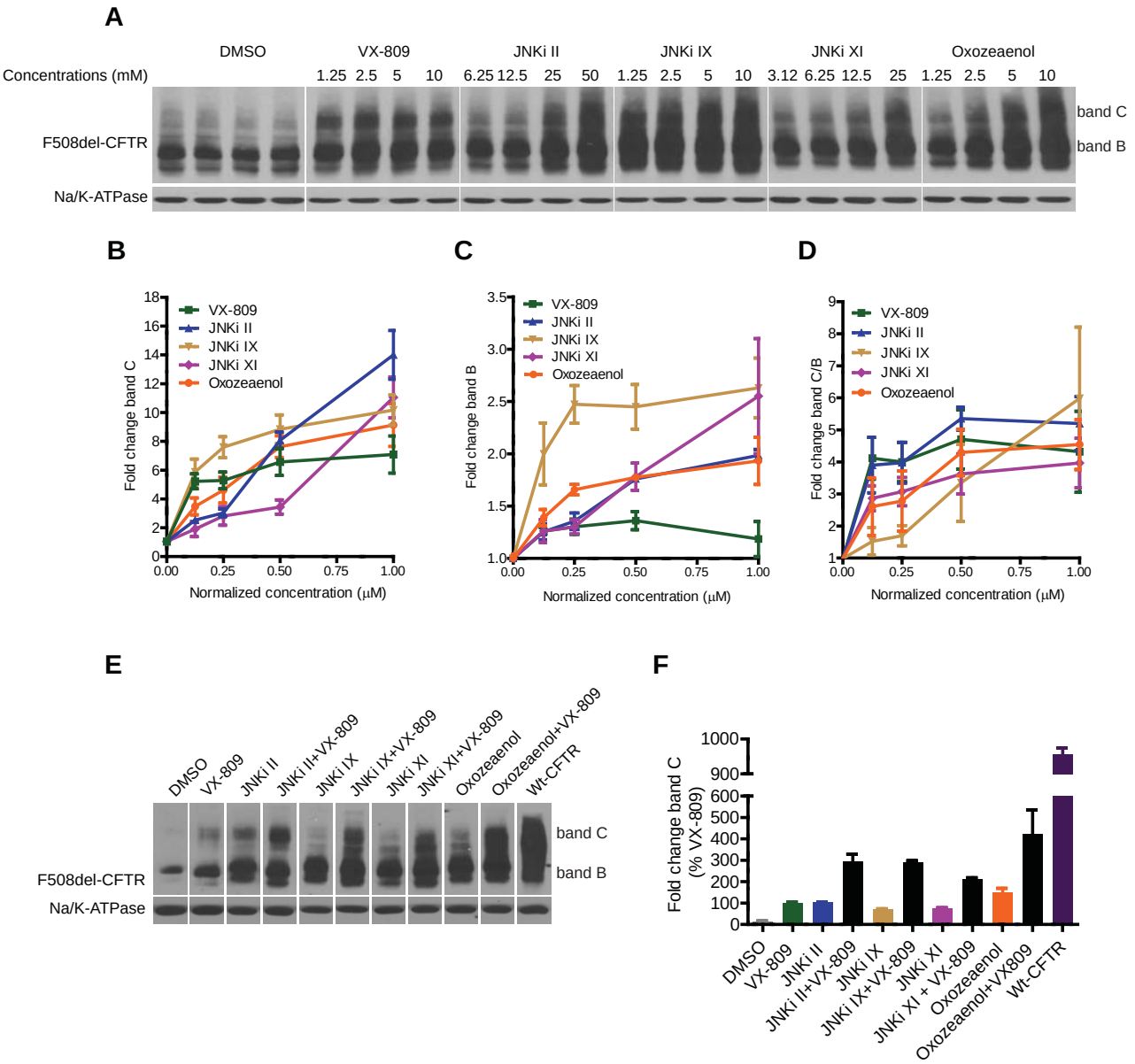
A
DMSO
VX-809
JNKi II
JNKi IX
JNKi XI
Oxozeaenol
Concentrations (mM)
1.25 2.5 5 10
6.25 12.5 25 50
1.25 2.5 5 10
3.12 6.25 12.5 25
1.25 2.5 5 10
F508del-CFTR
band C
band B
Na/K-ATPase
B
Fold change band C
Normalized concentration (μM)
C
Fold change band B
Normalized concentration (μM)
D
Fold change band C/B
Normalized concentration (μM)
VX-809
JNKi II
JNKi IX
JNKi XI
Oxozeaenol
E
DMSO
VX-809
JNKi II
JNKi II+VX-809
JNKi IX
JNKi IX+VX-809
JNKi XI
JNKi XI+VX-809
Oxozeaenol
Oxozeaenol+VX-809
Wt-CFTR
F508del-CFTR
band C
band B
Na/K-ATPase
F
Fold change band C (% VX-809)
DMSO
VX-809
JNKi II
JNKi II+VX-809
JNKi IX
JNKi IX+VX-809
JNKi XI
JNKi XI + VX-809
Oxozeaenol
Oxozeaenol+VX809
Wt-CFTR